Petrogenesis of late Ediacaran volcanic rocks of the Kerdous and Tagragra d'Akka inliers (anti-atlas Morocco): Involvement of slab-failure

Olivier Blein, Thierry Baudin, Philippe Chevremont, Dominique Gasquet

Journal Pre-proof

Petrogenesis of late Ediacaran volcanic rocks of the Kerdous and Tagragra d'Akka inliers (anti-atlas Morocco): Involvement of slab-failure

Olivier Blein, Thierry Baudin, Philippe Chevremont, Dominique Gasquet

PII: S1464-343X(23)00004-3

DOI: https://doi.org/10.1016/j.jafrearsci.2023.104831

Reference: AES 104831

To appear in: *Journal of African Earth Sciences*

Received Date: 28 October 2022

Revised Date: 16 December 2022

Accepted Date: 5 January 2023

Please cite this article as: Blein, O., Baudin, T., Chevremont, P., Gasquet, D., Petrogenesis of late Ediacaran volcanic rocks of the Kerdous and Tagragra d'Akka inliers (anti-atlas Morocco): Involvement of slab-failure, *Journal of African Earth Sciences* (2023), doi: https://doi.org/10.1016/j.jafrearsci.2023.104831.

Petrogenesis of late Ediacaran volcanic rocks of the Kerdous and Tagragra d'Akka inliers (Anti-Atlas Morocco): Involvement of slab-failure

Olivier BLEIN[1], Thierry BAUDIN[1-2], Philippe CHEVREMONT[1], Dominique GASQUET[3]

[1] *BRGM, ISTO, UMR 7327, 3 av. Claude Guillemin, BP 36009, 45060 Orléans Cédex, France,* *o.blein@brgm.fr*

ORCID : 0000-0003-3514-9641

[2] *CNRS/ISTO, UMR 7327, 1A rue de la Férollerie, 45071 Orléans Cédex, France*

[3] *Université Savoie Mont Blanc, Laboratoire EDYTEM, UMR 5204 CNRS, Bâtiment Pole Montagne, Campus Scientifique, 73376 Le Bourget du Lac, France.*

Keywords. Anti-Atlas, Ediacaran, ignimbrite, silicic LIPs, slab failure.

ABSTRACT

Late Ediacaran rocks of the Ouarzazate Group define a thin pile of sediments and pyroclastic deposits between the Paleoproterozoic basement and the Cambrian sedimentary cover in the southern Kerdous and Tagragra d'Akka inliers. In the Tafeltast area, terrigenous sediments with volcano-sedimentary and pyroclastic rocks are located in grabens controlled by syn-sedimentary normal faults. The sedimentation is characterized by a maximum flooding outlined by the Agoujgal carbonates. In the Tagragra-n-Daouizid, the Ouarzazate Group represents the surficial emission of rhyolitic pyroclastic flows. This pyroclastic activity was associated with continental coarse-grained sedimentary deposits. In the Tagragra Ouahallal, the volcanic sequence is comparable to that observed in subglacial volcanoes. Massive ash layers, intrusive pillow lavas in waterlogged deposits, stacking of lava flows, alternation of emerged and submerged periods under shallow water, are characteristics described in sub-glacial mafic volcanoes.

According to geochemical data, volcanic rocks of the Ouarzazate Group are: (i) mafic rocks with continental flood basalt and calc-alkaline basalt affinity; (ii) high-K calc-alkaline felsic rocks, generated by partial melting of crustal lithologies, or by an enriched mantle with involvement of crustal component; and (iii) intermediate to felsic slab failure rocks derived through mantle processes including melting of mafic upper portion of the subducted slab (Hildebrand and Whalen, 2017).

1. Introduction

In southern Morocco, the Anti-Atlas belt is characterized by inliers of Precambrian basement unconformably overlain by a late Ediacaran to Palaeozoic sedimentary cover (Fig. 1). This Precambrian bedrock is composed of: (1) Paleoproterozoic metamorphosed sediments and plutonic rocks; (2) Cryogenian oceanic volcano-sedimentary rocks affected by the Pan African tectonics; (3) Early Ediacaran continental volcano-sedimentary rocks affected by the last Pan African tectonic events; and (4) and Late Ediacaran voluminous pyroclastic rocks (Ouarzazate Group).

Geological mapping, petrographic, geochemical and geochronological studies indicate that Ediacaran volcano-sedimentary sequences consist of basaltic to rhyolitic lavas, dacitic to rhyolitic ignimbrite and volcaniclastic rocks of variable thickness (Choubert, 1963; Hassenforder, 1987; Ouguir et al., 1996; Youbi, 1998; Fekkak et al., 2000, 2003; Bajja, 2001; Piqué, 2003; Thomas et al., 2002, 2004; Gasquet et al., 2005, 2008; Walsh et al., 2012; Blein et al., 2014b; Karaoui et al., 2014, 2015; Errami et al., 2020; Yajioui et al., 2020). These deposits formed in active tectonic settings, such as a rift or more probably in transtensional and transpressional deformation zone (Doblas et al., 2002; Thomas et al., 2004; Gasquet et al., 2005, 2008; Blein et al., 2014b; Errami et al. 2020). Understanding of these essential felsic pyroclastic deposits highlights the late stage of the Pan-African orogeny.

Geological survey, within the framework of the Moroccan National Project of Geological Mapping (1/50,000 scale sheet map of Sidi Bou'addi, Tamazrar, Awkarda and Tlatat Ida Gougmar), gave opportunities to acquire new geological, geochemical, and geochronological data in the Kerdous massif and the Tagragra d'Akka (Chalot-Prat et al., 2001; Gasquet et al., 2001; Roger et al., 2005; Chèvremont et al., 2005). The volcanic and sedimentary deposits of the Ouarzazate Group crop out episodically between the Paleoproterozoic poly-structured basement and the Paleozoic sedimentary cover.

The objectives of this publication are: (i) a better constraint of the lithological units of the western Anti-Atlas; (ii) to present new petrographic and geochemical data on igneous rocks from the Tagragra d'Akka and the Kerdous-Tafeltast inliers; (iii) to compare the two inliers; and (iv) to discuss the geodynamical context at the end of the Ediacaran.

2. Regional setting

South of the South Atlas Fault, the Anti-Atlas belt is subdivided into three geographic domains (Fig. 1): (i) the western Anti-Atlas characterized by Paleoproterozoic metamorphosed sediments and plutonic rocks in the Bas Drâa, Ifni, Kerdous, Tagragra d'Akka, Tagragra de Tata, Zenaga, Iguerda, Agadir-

Melloul and Ighrem inliers; (ii) the central Anti-Atlas with Cryogenian island-arc – basin sequences in the Sirwa massif and the Bou-Azer Inlier; and (iii) the eastern Anti-Atlas with thick Ediacaran volcano-sedimentary sequences in the Saghro massif and the Ougnat inlier (Ennih and Liégeois, 2008).

Within the Kerdous-Tafeltast and Tagragra d'Akka inliers (Fig. 1), Precambrian rocks have been divided in five main lithological units, corresponding to major geodynamic events: (1) Paleoproterozoic metasedimentary schists, (2) Paleoproterozoic plutonic suites, (3) late Paleoproterozoic-Mesoproterozoic sediments, (4) Ediacaran volcano-sedimentary and volcanic rocks, and (5) a late Ediacaran - early Cambrian sediments.

2.1. Paleoproterozoic rocks

The Paleoproterozoic basement crops out in several inliers (Fig. 1; Ifni, Ighrem, Kerdous, Zenaga, Tagragra d'Akka etc.), and is composed of metamorphic and magmatic rocks (Aït Malek et al., 1998; Thomas et al., 2002; Walsh et al., 2002; Blein et al., 2022). The metamorphic rocks consist of greenschist to amphibolite facies siliciclastic rocks and migmatites (Zenaga Group). The metasedimentary rocks are fine-grained sandstones with interbedded volcanic layers. In the Tagragra de Tata inlier, felsic metatuffs have been dated at 2072±8 Ma (Walsh et al., 2002). In the Kerdous inlier, metamorphosed siliciclastic sediments are intruded by Rhyacian (2187±33 Ma, O'Connor, 2010; 2106±12 Ma, Blein et al., 2022) and Orosirian granitoids (ca. 2.04-2.06 Ga, Gasquet et al., 2004; O'Connor, 2010). According to Nd model ages (Mrini, 1993; Mortaji et al., 2000), the source of these siliciclastic sediments is Archean.

Two main Orosirian plutonic events led to the intrusion of (Gasquet et al., 2008; Blein et al., 2022): (i) a calc-alkaline suite composed of diorites, monzodiorites, granodiorites and granites originating from a mantle source with involvement of crustal material (Azguemerzi Suite); and (ii) peraluminous granites and leucogranites originating from a crustal source (Tazenakht Suite) into the metamorphosed siliciclastic rocks.

2.2. Proterozoic sediments

From late Paleoproterozoic, the northern edge of the West African Craton is a passive margin which sediments, unconformably overlying the Paleoproterozoic basement, are termed the Lkest-Taghdout Group (Zenaga, Agadir-Melloul and Iguerda inliers; Thomas et al., 2002; Blein et al., 2013; Chèvremont

et al., 2013; Soulaimani et al., 2013), the Lkest Group (Kerdous inlier; BGS, 2001a, b) or the Tizi n'Taghatine Group (central Anti-Atlas; Bouougri and Saquaque, 2004). These sediments are quartzites, siltstones and stromatolitic carbonates, and were considered as Neoproterozoic, marking the opening of the Bou Azer ocean (Clauer, 1976; Bouougri and Saquaque, 2004; Thomas et al., 2004). However, this assumption is now questioned since detrital zircon ages of these sediments point to a maximum age of deposition around 1.8 to 1.7 Ga (Abati et al., 2010; Soulaimani et al., 2019). This age estimate is corroborated by age determinations on baddeleyite and zircon ages of crosscutting mafic sills and dykes (ca. 1.71 Ga: Ikenne et al., 2017, Youbi et al., 2013; ca. 1.63 Ga: Kouyate et al., 2013, Aït Lahna et al., 2020), and on pegmatites (ca. 1.76 Ga: Gasquet et al, 2004).

2.3. Ediacaran sedimentary and magmatic events

During Lower Ediacaran (before 580 Ma), volcano-sedimentary rocks are known as the Saghro Group (central and Eastern Anti-Atlas), the Anezi series (western Anti-Atlas), the Tiddiline Group (central Anti-Atlas), and the Bou Salda Group (eastern Anti-Atlas). During Upper Ediacaran (after 580 Ma), volcano-sedimentary rocks associated with high-level granites are known as the Ouarzazate Group throughout the entire Anti-Atlas.

Extending from the Sirwa to Ougnat massifs, the Saghro Group is composed of ca. 6000 m thick of deformed turbidites; the sedimentary cycles tend to be composed of shales, siltstones and sandstones that coarse upward, with carbonates (Thomas et al., 2002; Fekkak et al., 2003; Eddif et al. 2007; Pelleter et al., 2007; Michard et al., 2017). Recent U-Pb datations on detrital zircons characterized a maximum depositional age of 604±5 Ma (Errami et al. 2020).

Volcano-sedimentary rocks of the Anezi-Tiddiline-Bou Salda Group were deposited in subsident narrow grabens lined to a transtensive context (Thomas et al., 2004; Blein et al., 2014a). Felsic ignimbrites of the Bou Salda and Tiddiline groups have given U-Pb zircons ages of ca. 607–605 Ma (Thomas et al., 2002; Blein et al., 2014a). These volcano-sedimentary rocks deposits have been deformed between thses last ages and ca. 580 Ma, and unconformably overlain by pyroclastic flows of the Ouarzazate Group (Blein et al., 2014a).

Upper Ediacaran rocks (post 580 Ma) comprise sedimentary, volcano-sedimentary, pyroclastic and volcanic rocks, with locally sub-volcanic granitic rocks. Pyroclastic and volcanic rocks have high-K calc-alkaline to shoshonitic affinities, and plutonic rocks are essentially I- and S-type granitoids, with local A-

type granitoids intrusions (Thomas et al., 2002; El Baghdadi et al., 2003; Gasquet et al., 2005; Errami et al., 2009; Toummite et al., 2012; Walsh et al., 2012; Blein et al., 2014b; Baidada et al., 2017; Belkacim et al., 2017). U-Pb zircon ages for these intrusions range between ca. 575–542 Ma (Hawkins et al., 2001; Cheilletz et al., 2002; Walsh et al., 2002; Gasquet et al., 2005; Blein et al., 2014a, b; Karaoui et al., 2015). In the Central Anti-Atlas, the large variations in the thickness of the Ouarzazate Group are controlled by a pronounced paleo-relief. These volcano-sedimentary rocks are locally affected by syn-sedimentary deformation (SE striking folding and NE-SW faulting; Blein et al., 2014b),

In the Central Anti-Atlas, the important thickness variations of the volcaniclastic Ouarzazate deposits are controlled, at the first order, by an accented horst and graben paleogeography (Blein et al., 2014b). Moreover, the successive volcaniclastic deposits are also linked to a syn-sedimentary tectonic event such as NW-SE striking folding and NE-SW faulting (Blein et al., 2014b), suggesting contemporaneous compressive and extensive zones in a transtensional regional context.

Two main geodynamic contexts have been proposed for the magmatisme of the Ouarzazate Group: (i) subduction related (Bajja, 1998; El Baghdadi et al., 2003; Benziane, 2007; Walsh et al., 2012; Hefferan et al., 2014); or (ii) post-collisional with respect to the Pan-African arc-continental main collisional event (Thomas et al., 2002; Gasquet et al., 2005, 2008; Toummite et al., 2012). Blein et al. (2014a, b) have proposed an origin linked to a slab breakoff that occurred between ca. 580–575 Ma. The subsequent magmatism following slab breakoff is felsic, and results from partial melting of continental crust.

2.4. Late Ediacaran to Cambrian sedimentation

The Late Ediacaran volcanic and volcano-sedimentary rocks of the Ouarzazate Group are unconformably overlain by a thick carbonate to clastic sedimentary cover comprising from bottom to top: (i) the transgressive late Ediacaran to early Cambrian Taroudannt Group, (ii) the Cambrian Tata Group, and (iii) the Cambrian to Ordovician transgressive groups of internal Feijas, Tabanite, external Feijas, and Ktaoua. The Taroudannt Group is composed by the carbonate-dominated Adoudou Formation and the terrigenous-carbonate-dominated Taliwine Formation, which is dominantly carbonate westward and exclusively terrigenous further east (Choubert, 1952, 1953a, b). Carbonates of the Adoudou Formation have microbial origin structures, and characterize a regional subsidence context responsible for the progressive flooding of the Anti-Atlas, from West to East (Boudda et al., 1979; Geyer, 1990; Benssaou and Hamoumi, 2001; Alvaro et al., 2005, 2014). Locally, volcanic lavas occur interbedded within

sediments of the uppermost part of the Adoudou Formation. This context is interpreted as continental rifting (Piqué et al., 1999; Benssaou and Hamoumi, 2001, 2003; Soulaimani et al., 2003).

U/Pb age determinations from the Boho volcano (529±3 Ma; Ducrot and Lancelot, 1977) and from the Aghbar trachyte sill (531±5 Ma; Gasquet et al., 2005) suggests a Cambrian age for the Adoudou Formation, in which they are interlayered. Recently, an older U-Pb late Ediacaran age (542±5 Ma; Blein et al., 2014b) has been obtained on volcanic breccia at the base of the Adoudou Formation.

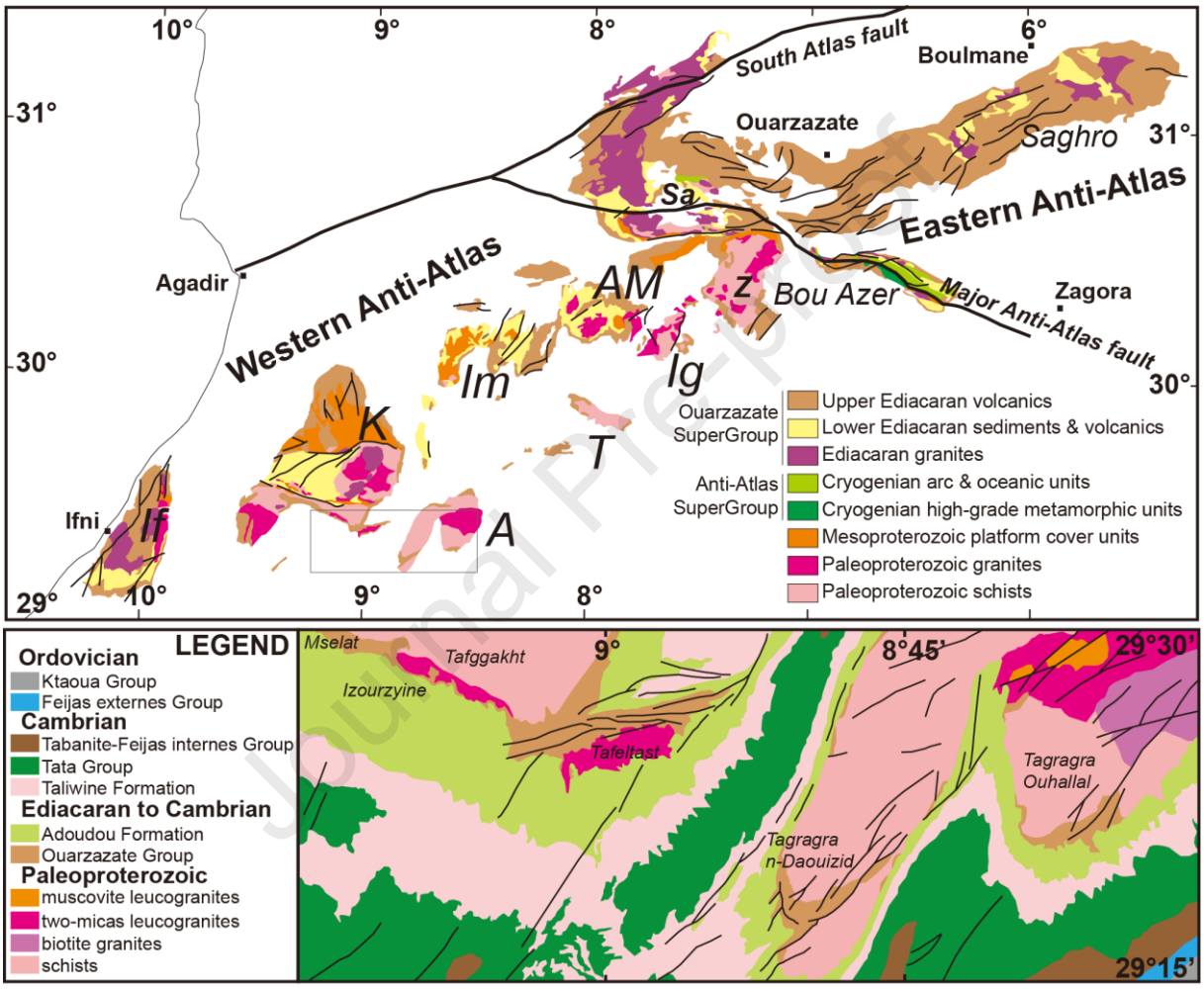

Figure 1: Precambrian geology of the Anti-Atlas inliers (modified from Hollard et al.1985, Walsh et al. 2002, and Gasquet et al. 2008). A: Tagragra d'Akka; AM: Agadir-Melloul; BD: Bas Drâa; If: Ifni; Ig: Iguerda; Im: Igherm; K: Kerdous; Sa: Sirwa; T: Tagragra de Tata).

3. Field relationships and petrography

Geological mapping, carried out within the National Geological Mapping Plan of Morocco, allows to establish a new lithostratigraphic chart of the Proterozoic rocks (Thomas et al., 2004). In discontinuity with the Anti-Atlas Supergroup (800-680 Ma), the Ouarzazate Supergroup (615-542 Ma) is characterized by continental deposits and post-orogenic magmatism accumulates in a graben system. The Ouarzazate Group defined on the present Awkarda map sheet, as well as on the eastern sheets of Sidi Bou'addi and Tamazrar is the upper part of the Ouarzazate Supergroup defined by Thomas et al. (2004). In the entire Anti-Atlas, the deposits of the Ouarzazate Group are included in an age range between ca. 575–542 Ma (Hawkins et al., 2001; Cheilletz et al., 2002; Walsh et al., 2002; Gasquet et al., 2005; Blein et al., 2014a, b; Karaoui et al., 2015).

The Ouarzazate Group is mainly composed of fluvial-lacustrine deposits accumulated in small basins bordered by high levels (Tagragra Ouhallal, Tagragra-n-Daouizid, Tafeltast, and south of Zawyat-n-Dougadir; Fig. 1). This sedimentation is contemporary with volcanic and pyroclastic flows. Volcanic and sedimentary deposits accumulate on the margin of narrow grabens, and exhibit high lateral and upward variations. Volcanic and sedimentary rocks are sub-conformably overlain by the late Ediacaran sediments of the Adoudou Formation.

3.1. Kerdous inlier

In the Tafeltast area, the Ouarzazate Group is composed of sediments with few volcano-sedimentary rocks, and high vertical and lateral variations (Figs. 2A and 3), with a thickness ranging between 0 to 250 m. Volcano-sedimentary deposits are located in a NE striking narrow half-graben controlled by syn-sedimentary normal faults. The NW limit is a SE dipping normal fault, and the SE limit is the top of a tilted block. The Ouarzazate Group is conformably overlain by late Ediacaran marine sediments (Adoudou Formation), which are contemporaneous with a less and less active syn-sedimentary extensive tectonism.

The Ouarzazate Group sediments were deposited in a fluvial-lacustrine setting in a tectonic and magmatic active system. The fluvial-lacustrine sediments unconformably overlie the Paleoproterozoic basement with a basal sedimentary breccia. This breccia rapidly evolves laterally and upward to finer silts (the lower silts facies, Fig. 3). The vertical aggradation of the rapid limit between breccia and siltstone indicates a progressive deepening of the graben during the Upper Ediacaran. In the middle of the sedimentary pile, breccia and silts are overlain by a carbonate sedimentation, the Agoujgal carbonates (a carbonate key bed), which marks a maximum flooding (Figs. 2A and 3).

This lacustrine sedimentation presents therefore a complete transgressive and regressive cycle. The basal and lateral breccia reaches one to 20 m thickness and includes heterometric blocks of Paleoproterozoic basement: schist, quartzite, gabbro, dolerite and granite. The petrography of the blocks reflects the lithology of the closer Paleoproterozoic basement, suggesting a very limited transport of sediments. Two types of breccia may be mapped: breccia with schists or granite dominant blocks.

The basal breccia with Paleoproterozoic schist blocks outlines the northern border of the Ediacaran graben (Fig. 2A). The clasts, angular and unclassified, suggest a limited transport. Volcanic lenses stratified in these breccias outline the occurrence of a contemporaneous volcanism. The Paleoproterozoic basement is often affected by metric faulting zones with tectonic breccias. The progressive change from tectonic to sedimentary breccias suggests that the first feeds the second. Basal breccias are related to the development of normal faults which are at the origin of the Ediacaran grabens.

The basal breccia with Paleoproterozoic granite blocks outlines the southern limit of the Upper Ediacaran graben (Fig. 2A). Breccias result from reworking of a granitic arena on a slight slope dipping to the north, and are pinching out to the south. Then, the Paleoproterozoic basement is overlain by the last volcanic flows of the Ouarzazate Group, or by the sediments of the Adoudou Formation. This setting suggests the existence of paleo-relief with horst structure composed of Paleoproterozoic basement to the south.

The Agoujgal carbonates, representing a maximum flooding surface, are a key bed in the Ediacaran sedimentary sequence of the Tafeltast area. The number and thickness of carbonate levels increase from the southern border to the middle of the basin. In the central part of the basin, six carbonate levels with a decreasing thickness from 25 to 3 meters have been observed. The basal carbonate level crops out from the southern border to the center of the basin. The Agoujgal Formation is characterized by the following stratigraphic facies: i) the basal calcareous of Agoujgal; ii) alternating between carbonate, siltstone and volcanic rock; and iii) alternating between carbonate, conglomerate and volcanic rock. The two latter associations are contemporaneous. They overlie the basal carbonate level. The Agoujgal carbonates are composed of light dolosparite stratified in decimetric beds. This lithofacies is characterized by an algo-bacterial lamination, that is often silicified, and quartz-rich fine layers. Few rhyolitic lenses are interbedded in these carbonates.

Alternating carbonates, siltstones and volcanic rocks (metric to decametric thickness) mark the beginning of the regressive interval which results in a decreasing number, extension and thickness of the carbonate levels in favor of the silty terrigenous sedimentation. Towards the top, carbonates and volcanic rocks tend to disappear, giving way to the purely terrigenous sedimentation of the upper siltstones.

On the southern edge of the graben, siltstones are laterally replaced by conglomeratic deposits, which prograde and end up the upper conglomerates. Interlayered and lenticular volcanic emissions occur as lava flows, ignimbrites or block lava flows.

Volcanic deposits are localized on the emerging borders of the basin, and in lenses interbedded in the sediments of the Agoujgal Formation (Figs. 2A and 3). Volcanic rocks are basaltic lavas flows or rhyolitic pyroclastic deposits, with limited geographic extension. All the emission centers rest on the Paleoproterozoic granitic basement. Volcanic deposits are overlain by the last sequence of the upper conglomerates or by the basal deposits of the Adoudou Formation. The volcanic activity was locally still active until the basal deposits of the Adoudou Formation. This mafic volcanism is latter than one which outcrops in the Tagragra Ouhallal area localised than SE. Basalts have microlitic to intersertal, more or

229 less porphyritic textures with the following mineralogy: feldspar, oxides, apatite, sericite, chlorite, calcite,
230 hydroxides with sometimes the asserted presence of altered olivine.

231 Rhyolitic pyroclastic flows form an east-west trending crest that joins the north of Mselat to the peaks
232 east of Tafggakht. They are marked in the landscape by a multi-decameter alternation of white and dark
233 colors despite their comparable chemistry. The dark color could be the result of a higher proportion of
234 glass in the matrix. Pyroclastic flows are locally separated by lapilli tuffs of multi-decimetrer thickness.
235 North of Mselat, the first volcanic level is a dark brecciated glass-clastic tuff that flows over basal
236 breccias with dominant granitic elements about 15 metres thick; the latter resting on Paleoproterozoic
237 schists. To the east and south of Tafggakht, the Paleoproterozoic granite is directly overlain by an
238 ignimbritic bedded rhyolite. These rhyolitic deposits are almost entirely covered by the upper
239 conglomerates. These conglomerates are characterized by - locally metric - rhyolitic blocks.

240 The second rhyolitic flow to the NE of Mselat, about 50 m thick, was U/Pb dated on zircon by the
241 SHRIMP method and provided an age of 561±6 Ma (Chèvremont et al., 2005). This porphyritic rhyolite
242 shows a fluid glass-clastic texture with phenocrysts of feldspar, quartz, oxides, sericite, pumpellyite, and
243 micro-lapilli.

244 Andesitic to dacitic pyroclastic flows cap the tops of the Izourzine cliff and are clearly visible, with their
245 dark color contrasting with the light granite. They lie directly on the Paleoproterozoic granite and often
246 show flat- or cross-bedded ash cloud surge figures that outline gully channels and ash levels. This type
247 of structure is reminiscent of ash cloud deposits. These deposits are directly surmounted by the upper
248 conglomerates with rolled pebbles, and without volcanic elements.

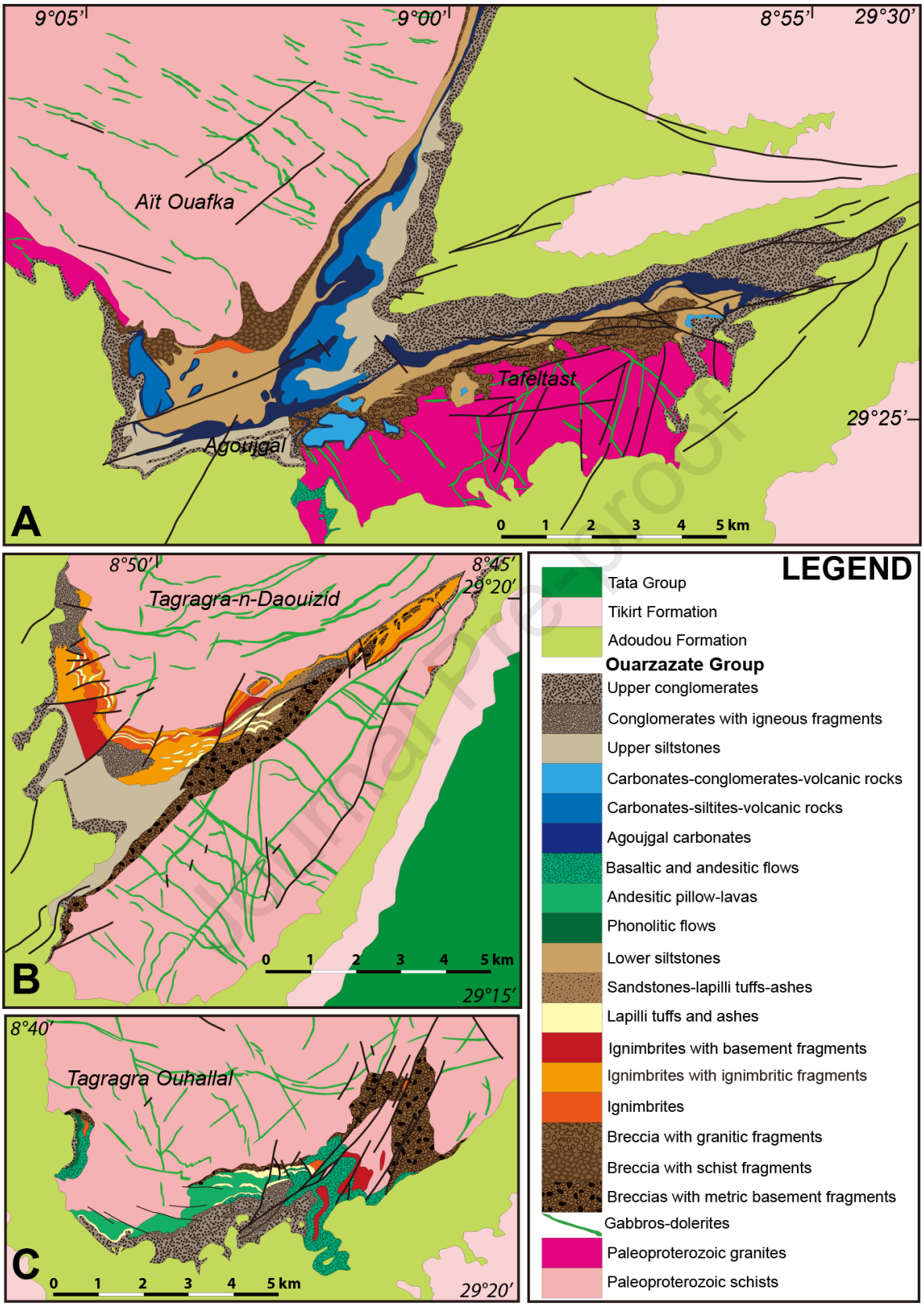

Figure 2: Simplified geologic maps: **A.** the Kerdous inlier (Baudin et al., 2005; Hassenforder et al., 2001); **B.** the Tagragra-n-Daouizid area (Hassenforder et al., 2001); and **C.** the Tagragra Ouhallal area (Roger et al., 2001).

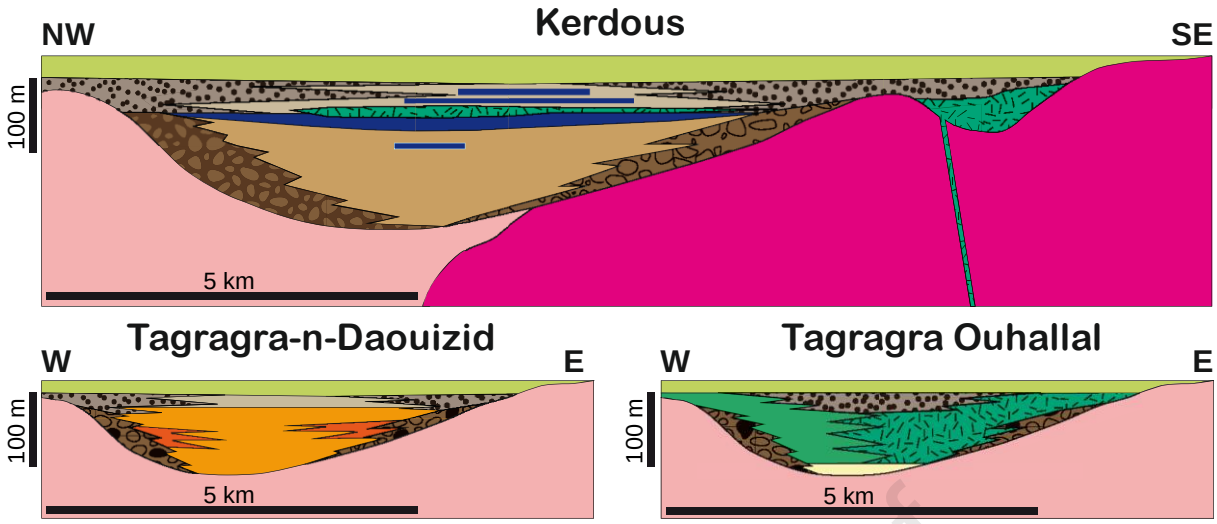

Figure 3: Schematic distribution of the different lithostratigraphic units. Symbols as in Fig. 2.

3.2. Tagragra-n-Daouizid area

In the Tagragra-n-Daouizid area, the Ouarzazate Group is composed of conglomerates, volcano-sedimentary rocks with pyroclastic rocks, and high vertical and lateral variations (Fig. 2B), with a thickness ranging between 0 to 100 m. The basal chaotic breccias are characterized by heterometric and heterolithic blocks, essentially substrate-derived rocks such as schist, granite, quartzite, dolerite and gabbro (Figs. 2B and 3). The lithology of the clasts reflects the lithology of the local basement, the distance of transport of clasts was limited. The breccias are observed at the base of clast-rich ignimbrites which beginning the volcanic sequence. These breccias are not restricted to the base of the volcanic sequence, they also crop out stratified in the middle and at the top of the volcanic sequence. They are related to fault-controlled scarps which were activated prior to volcanic eruptions. The regular occurrences of these chaotic breccias suggest that the faults were still active during all the volcanic activity.

Sandstones stratified with lapilli tuffs and ashes are well established in the center of the volcano-sedimentary sequence. Sandstones are light, fine to middle grained, and quartz-feldspathic in composition. Stratified in beds, they are covered without transition with a few meter thick of chaotic breccias observed at the top of an ignimbritic unit, and alternate regularly with well stratified tuffs. These sandstones are river deposits in shallow water. The rapid change between breccias and sandstones, suggest that the formation of the breccias is independent from the river system which control the sandstone deposits.

On top, the Ouarzazate Group is characterized by pelitic facies such as silts. These silts are interbedded with micro-conglomeratic sandstones which are more abundant at the top of the sedimentary sequence (Figs. 2B and 3). These silts overlie conformably ignimbrites, conglomerates and breccias, and constitute a lenticular lens in the central part of the grabens. Silts are certainly lake deposits, and mark the end of pyroclastic density currents such as ignimbrites. The deposits herald the end of the maximum basement deformation. However, ash fall deposits and coarse grained sandstones occur locally.

The youngest deposits of the Ouarzazate Group are polygenic conglomerates and coarse-grained sandstones, with a large geographic extension overlying previous sedimentary and pyroclastic rocks and the Paleoproterozoic rocks.

Ediacaran volcanism is characterized by numerous pyroclastic flows. Massive lapilli tuffs with basement blocks overlie the Paleoproterozoic basement, chaotic breccias or basal conglomerates. Basement blocks are derived from collapse or erosion of the eruption conduit or substrate by the density current. These massive lapilli tuffs are non-welded, with little sub-rounded blocks which do not exceed one centimetre in size. This lithofacies lacks internal stratification and comprises pumice, lithic lapilli, and crustal fragments with a matrix of vitric ashes with crystals clasts. The thickness of volcanic deposits is variable (a few m to 30 m maximum).

Massive homogenous welded pyroclastic tuffs cover the massive lapilli tuffs with basement blocks. This ignimbrite forms massive, lenticular, 5 to 10 m thick layers, with a prismatic flow, often associated with a planar flow. They are interbedded with inframetric layers of lapilli and ash tuffs or embedded within thicker deposits of block ignimbrites. These ignimbrites have a vitroclastic texture, mostly unwelded and uncompacted, with 40% splinters and pumice fragments in an ashy matrix. Some horizons have a welded and hot compacted eutaxitic texture including a significant proportion of flames or compacted pumice fragments. The lack of basement xenoliths and the great homogeneity of the material explain the very frequent prismation of the deposits. The low frequency of welded tuffs means that the pyroclastic flows have a relatively moderate temperature at the time of flow immobilization.

Ignimbrites may contain 20 to 50% of angular blocks of massive ignimbrite of very variable size. The embedded blocks come from the pulverization of the older ignimbritic levels. The small width and considerable number of interlocking channels suggest the successive and extremely rapid emission of pyroclastic flows involving small volumes of magma.

Numerous fallout deposits, such as lapilli tuffs or ashes, are associated with the co-ignimbrite ash flow. They are generally black, green or purplish grey rocks, and are fine- to medium-grained, relatively homogeneous because they are always well sorted and locally with visible normal grading. They contain 40-50% volcanic fragments (crystal clasts; shredded pumice fragments), and angular xenoliths of Paleoproterozoic basement, all in a matrix of very fine, siliceous ashes.

3.3. Tagragra Ouhallal area

In the Tagragra Ouhallal area, the Ouarzazate Group outcrops locally between the Paleoproterozoic rocks and the late Ediacaran – Cambrian sediments, with a thickness ranging between 0 to 100 m (Figs. 2C and 3).

The volcanic sequence, highly diversified, consists of a succession of massive flows or pillow basalts of alkaline mafic lava, and lapilli tuffs and ashes, all locally preceded by deposits of dacitic to rhyolitic ignimbrites. All eruptions are continental and lenticular in nature. The sedimentary deposits consist of accumulations of breccia with basement fragments, which are interbedded with conglomerate and sandstone at the end of the volcanic sequence. The internal organization of the volcanic succession is quite simple although it is different from east to west.

To the east, lava flows overlain unconformably the basement, breccias, and ignimbrites. These flows may be overlain by breccia. Flows are massive, and interstratified with lapilli tuffs and ashes. Lavas are porphyritic, and or microlitic and fluidal, with plagioclase and clinopyroxene and olivine.

In the western part, tubular and pillow lavas make up the bulk of the volcanic sequence. They cover either the basement, basement breccia, or massive non-layered cinerites. The first pillow lavas are secant and intrusive in finely layered lapilli tuffs and ashes. Above, pillows and tubes form extrusive lenticular units interlayered with pyroclastic breccias, hyaloclastites and finely layered tuffs. These lavas were deposited under water. They are covered by breccia with basement fragments.

4. Geochemistry

Whole-rock major and trace elements were analysed by ICP-AES and ICP-MS (CRPG-CNRS, Nancy), respectively (Tables S1, S2, and S3). Sample preparation, analytical conditions and limits of detection are detailed in Carignan et al. (2001).

4.1. Kerdous inlier

Four lavas are mafic in compositions (SiO_2=39.3-52.6 wt%), with high Al_2O_3 (13.0-18.3 wt%) and TiO_2 contents (1.48-1.82 wt%), and low to high Fe_2O_3 (4.6-11.8 wt%), MgO (4.0-7.7 wt%), CaO (1.6-11.6 wt%), Na_2O (0.1-5.6 wt%), and K_2O contents (1.3-7.6 wt%; Fig. 4). Such variations on major elements are explained by a strong loss in ignition, which is generally higher than 3.5 wt%.

Basaltic flows display REE patterns with fractionated LREE ($2.1<[La/Sm]_n<4.3$), and slight or significant fractionation of HREE (Fig. 5A). The two basalts samples with the lower concentrations in LREE have $[Gd/Yb]_n$ ratios lower than 1.6. In contrast, the two other ones have fractionated HREE with $[Tb/Yb]_n$ ratios higher than 2.6. Normalized to Primitive Mantle values, their patterns display negative anomalies in Ta, Nb and Ti (Fig. 6A).

Three samples (AWTB27, AWTB78, and AWTB44-1) have andesitic composition (SiO_2=58.4-61.3 wt%), with high Al_2O_3 (17.0-17.8 wt%), and K_2O contents (3.9-8.8 wt%), low to high Na_2O contents (0.1-3.6 wt.%), moderate Fe_2O_3 (5.4-8.4 wt%), and low MgO (0.9-3.2 wt%), CaO (0.1-3.5 wt%) and TiO_2 contents (0.52-0.76 wt%; Fig. 4). These lavas are peraluminous with A/CNK ratio in the range 1.04–2.00, and show dominantly alkali, and magnesian to ferroan affinities (Fig. 7).

Intermediate lavas display REE patterns similar to basaltic lavas, with fractionated LREE ($3.5<La/Sm]_n<4.3$), slightly fractionated HREE ($1.5<[GdYb]_n<1.9$; Fig. 5B), and moderate negative Eu anomalies ($0.6<Eu/Eu^*<0.9$; Fig. 5B). The lack of significant HREE fractionation suggests that parent

liquids have been produced out of the garnet stability field. Intermediate lavas display systematic and high Ta, Nb and Ti negative anomalies relative to REE (Fig. 6B).

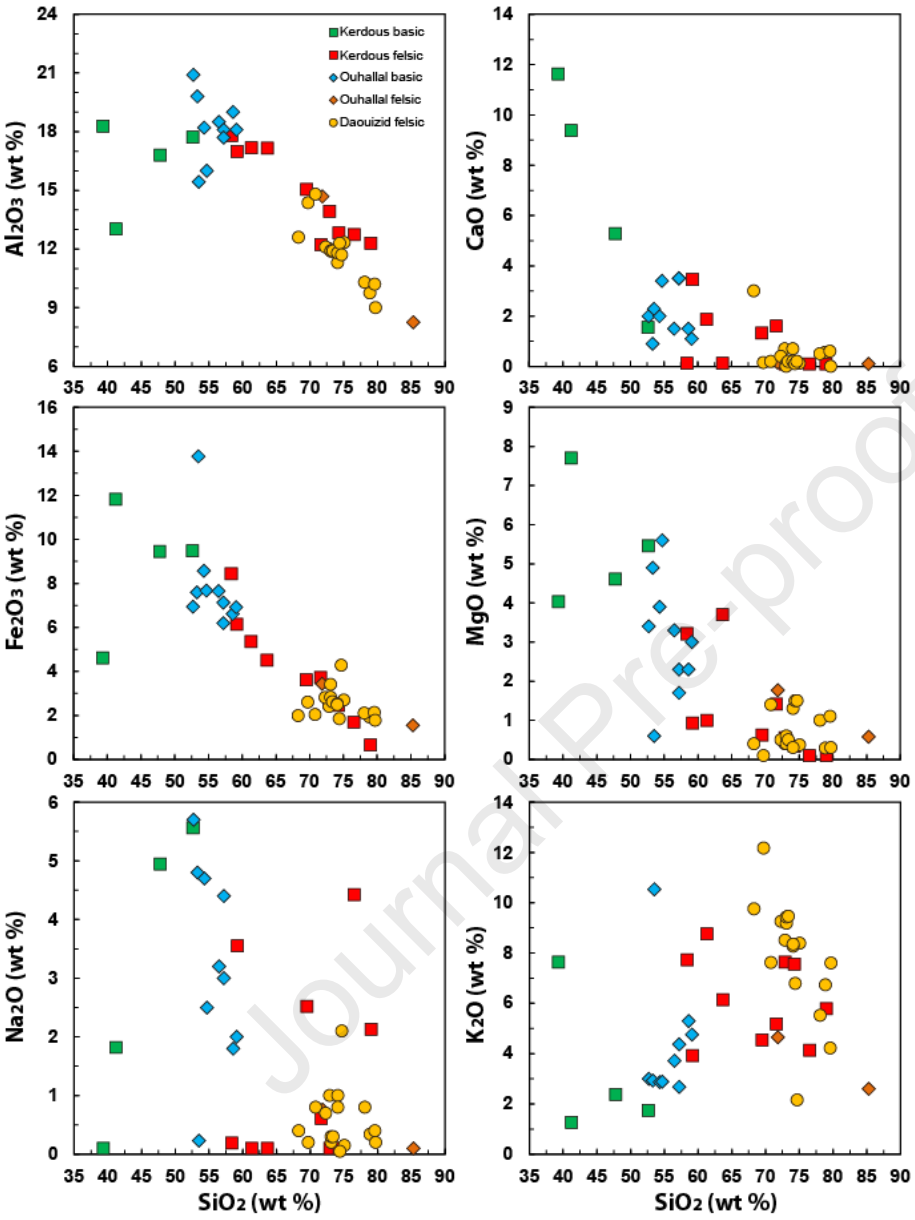

Figure 4: Harker diagrams for volcanic rocks from the Ouarzazate Group.

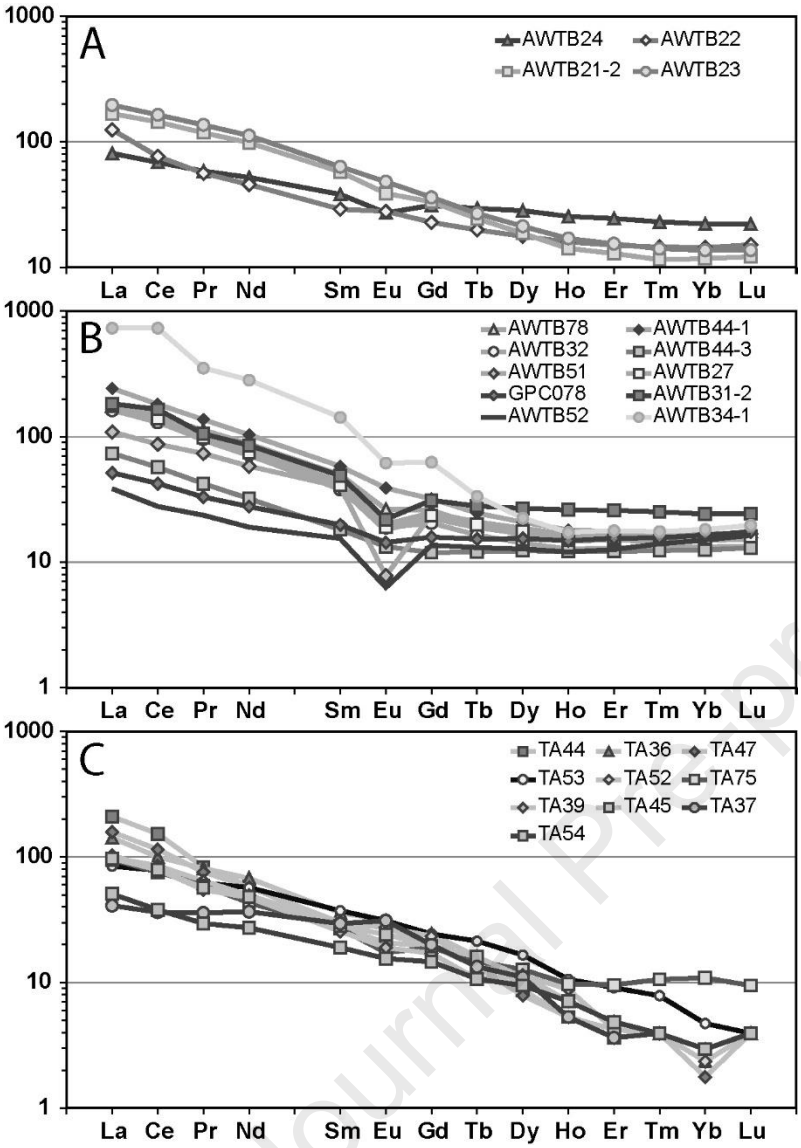

Figure 5: Chondrite normalized rare earth element diagram of volcanic rocks from the Kerdous inlier and the Tagragra Ouhallal area. **A.** Kerdous basalts & rhyolites; **B.** Kerdous intermediate and felsic volcanic rocks; **C.** Tagragra Ouhallal samples. Normalization according to Sun and McDonough, 1989.

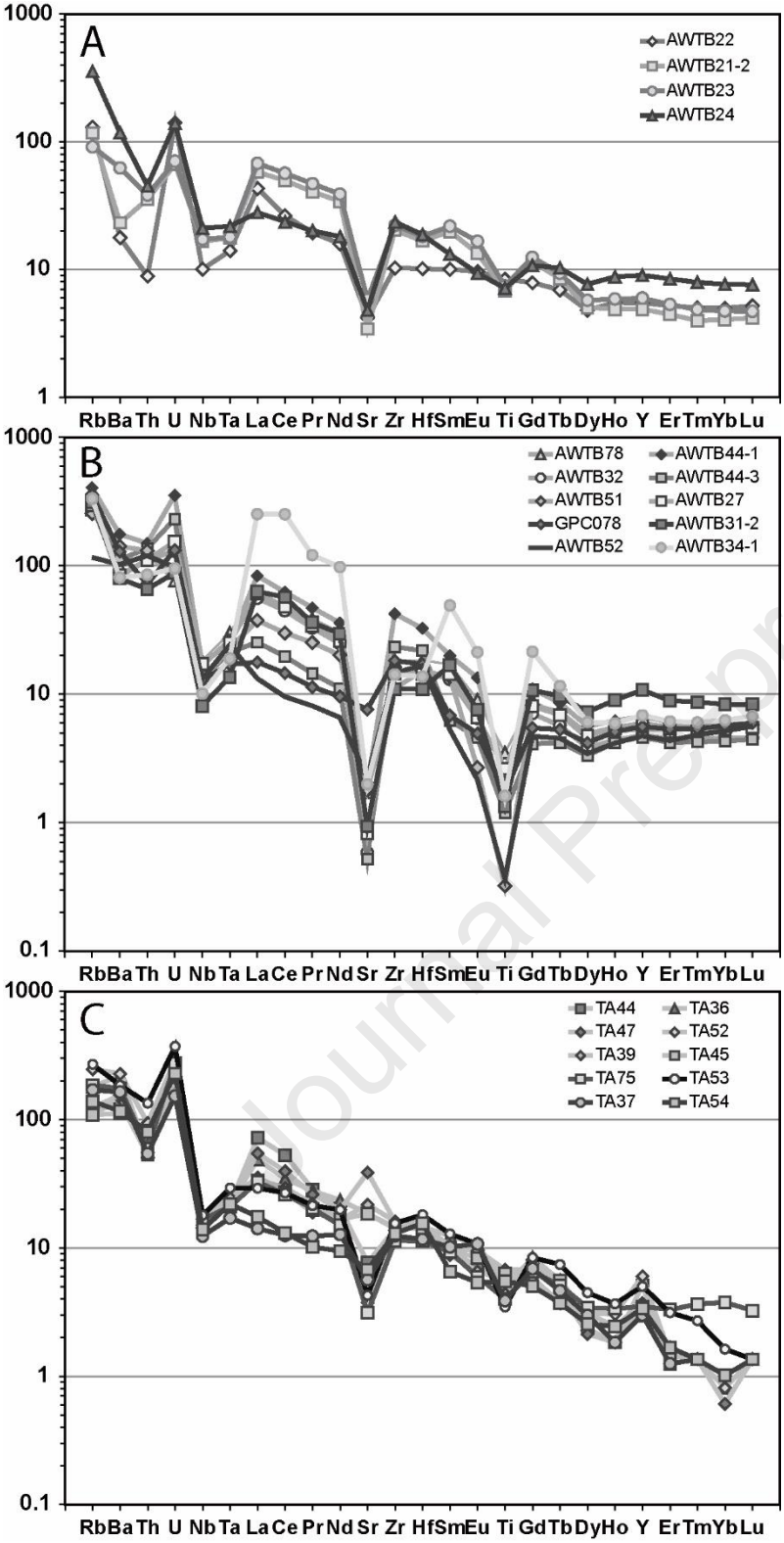

Figure 6: Primitive Mantle normalized multi-element diagram of volcanic rocks from the Kerdous inlier and the Tagragra Ouhallal area. **A.** Kerdous basalts & rhyolites; **B.** Kerdous intermediate and felsic volcanic rocks; **C.** Tagragra Ouhallal samples. Normalization according to Sun and McDonough, 1989.

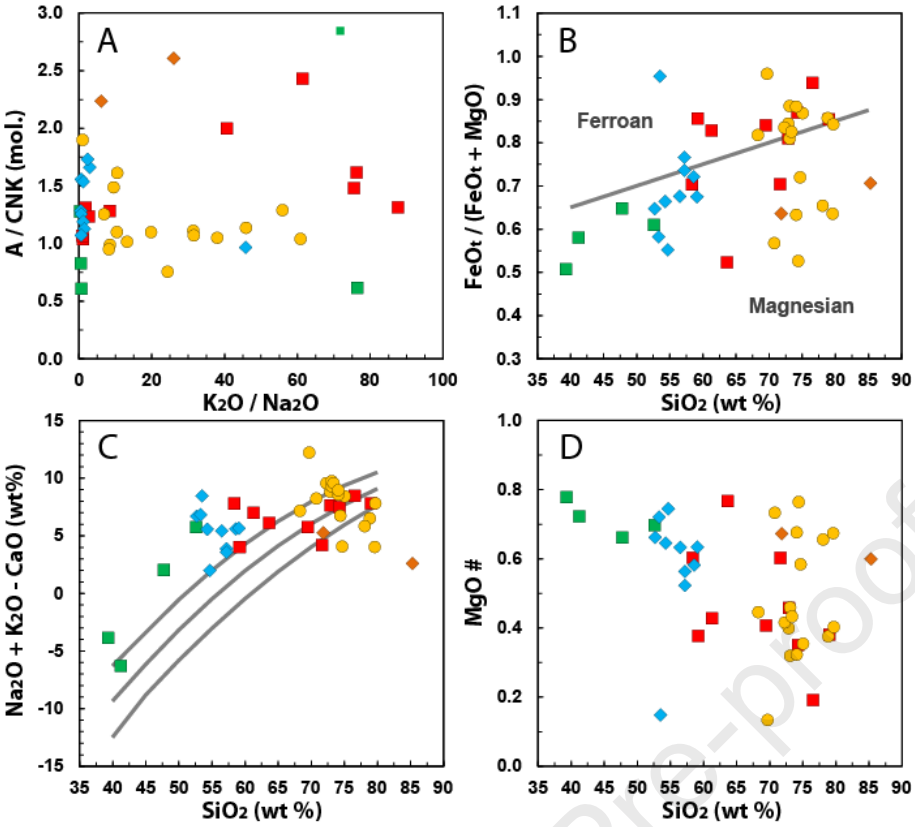

Figure 7: Major-element geochemistry of the Ouarzazate Group volcanic rocks. **A.** K_2O/Na_2O vs. A/CNK; **B.** SiO_2 vs. $FeO^t/(FeOt+MgO)$; **C.** SiO_2 vs. MALI index ($[Na_2O+K_2O]$-CaO) diagram of Frost et al. (2001); **D.** SiO_2 vs. Mg#. Symbols as in Fig. 3.

Few samples have dacitic to rhyolitic composition (SiO_2=63.7-79.0 wt%), with high Al_2O_3 (12.2-17.2 wt%), and K_2O contents (4.1-7.6 wt%), low to high Na_2O contents (0.1-4.4 wt%), and low Fe_2O_3 (0.7-4.5 wt%), MgO (0.1-3.7 wt%), CaO (0.1-1.6 wt%) and TiO_2 contents (0.07-0.57 wt%; Fig. 4). These lavas are peraluminous with A/CNK ratios in the range 1.03–2.47, and show dominantly alkali-calcic and magnesian to ferroan affinities. The K_2O/Na_2O ratios are higher than 1 (Fig. 7).

Rhyolitic lavas display REE patterns with fractionated LREE ($2.5<[La/Sm]_n<5.2$), with a high variability of LREE concentrations ($38<La]_n<730$), a lack of HREE fractionation and moderate to pronounced negative Eu anomaly ($0.2<Eu/Eu^*<0.9$; Fig. 5B). $[Gd/Yb]_n$ ratios are generally lower than 1.6, except for one sample (AWTB34-1; Fig. 5B). The high variability in LREE contents has not been observed in high field strength elements, then negative Ta- and Nb-anomalies are less important than for intermediate lavas. But negative Ti-anomaly is systematic and high (Fig. 6B).

4.2. Tagragra-n-Daouizid area

Rhyolites display major element compositions typical of potassic to high-potassic rhyolites with SiO_2 contents ranging between 69.7 and 79.7 wt%,. The high alkali concentrations (> 4 wt%) are essentially controlled by K_2O contents (2.2-12.2 wt%; Fig. 4). Na_2O concentrations are always lower than 1 wt%. These potassic to highly potassic rhyolites are characterized by negative correlations between SiO_2 and K_2O, and with Al_2O_3. The negative correlation between SiO_2 and K_2O may be related to the presence of Si poor and K rich minerals in the source such as ferriferous biotite and/or potassic and ferriferous amphibole.

Rhyolites display fractionated REE patterns, however four groups may be differentiated (Table 1). In the first group, $[La/Yb]_n$ ratios are higher than 20, with fractionated LREE ($2.7<[La/Sm]_n<8.9$) and HREE ($2.8<[Gd/Yb]_n<8.3$; Fig. 8A), and negative Eu anomalies. HREE contents are lower than 10 times chondrites. In the second group (TA5, TA2 and TA4), $[La/Yb]_n$ ratios are higher than 25, with fractionated LREE ($4.4<[La/Sm]_n<5.0$; Fig. 8B) and fractionated HREE ($2.8<[Gd/Yb]_n<4.5$), without negative Eu-anomalies. HREE contents are lower than 10 times chondrites (Fig. 8B). In the third group (TA85, TA11, TA12 and TA69A), $[La/Yb]_n$ ratios are lower than 18, with fractionated LREE ($3.0<[La/Sm]_n<4.1$) and slightly fractionated HREE ($1.6<[Gd/Yb]_n<3.0$), with light negative Eu anomalies. HREE contents are higher than 10 times chondrites (Fig. 8B). Finally in the fourth group, $[La/Yb]_n$ ratios are lower than 22, with fractionated LREE ($2.3<[La/Sm]_n<4.1$; Fig. 8C) and flat to slightly fractionated HREE ($0.9<[Gd/Yb]_n<2.9$). These samples are characterized by low REE contents ($\sum REE<60$ ppm).

In sample TA69A, the $[La/Yb]_n$ ratio is lower than 11, with fractionated LREE ($La/Sm]_n=4.1$) and slightly fractionated HREE ($[Gd/Yb]_n=1.6$), with slight negative Eu anomalies. This pattern is similar to sample TA85, suggesting that these two rhyolitic ignimbrites represent the same pyroclastic flow. In sample TA66A, the $[La/Yb]_n$ ratio is lower than 11, with fractionated LREE ($La/Sm]_n=3.0$) and slightly fractionated HREE ($[Gd/Yb]_n=2.0$), with light negative Eu anomalies. This pattern is similar to sample TA84, suggesting that these two rhyolitic ignimbrites represent the same pyroclastic flow.

In the Primitive Mantle normalizing diagram (Fig. 9), patterns display systematic negative anomalies in Ti and Sr, and sometimes in Nb and Ta.

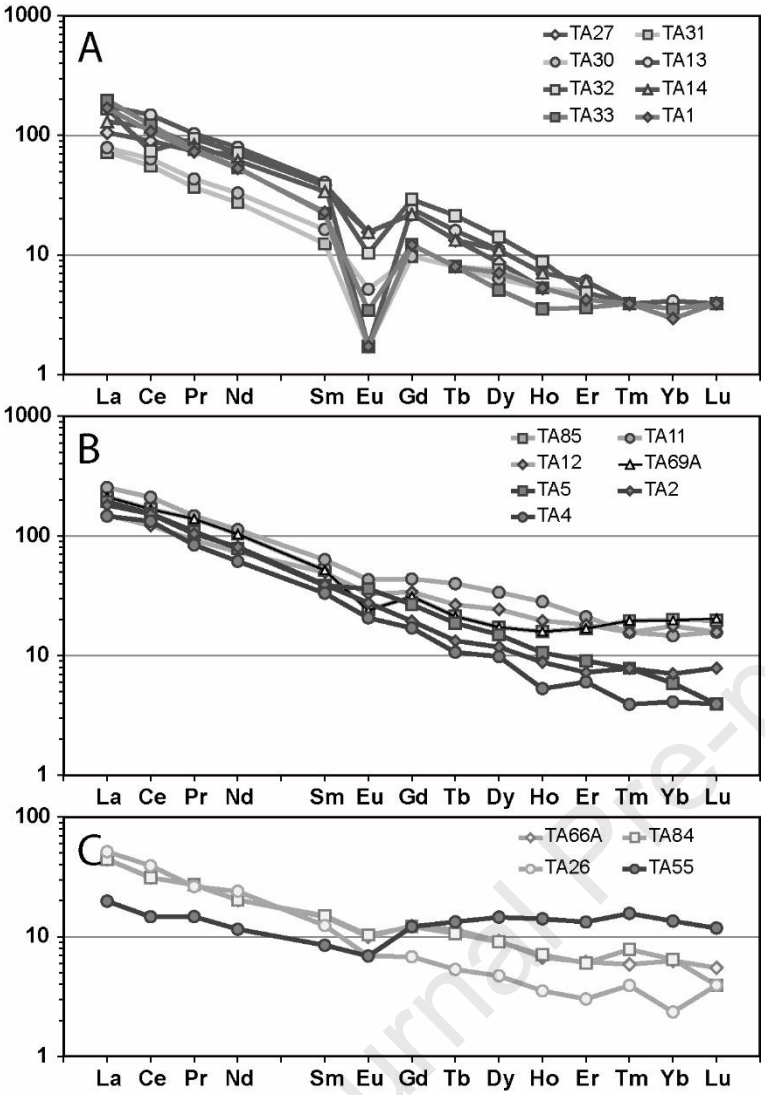

404

405 **Figure 8:** Chondrite normalized rare earth element diagram of volcanic rocks from the Tagragra-n-
406 Daouizid area. **A.** Group 1 rhyolites; **B.** Groups 2 and 3 rhyolites; **C.** Group 4 rhyolites. Normalization
407 according to Sun and McDonough, 1989.

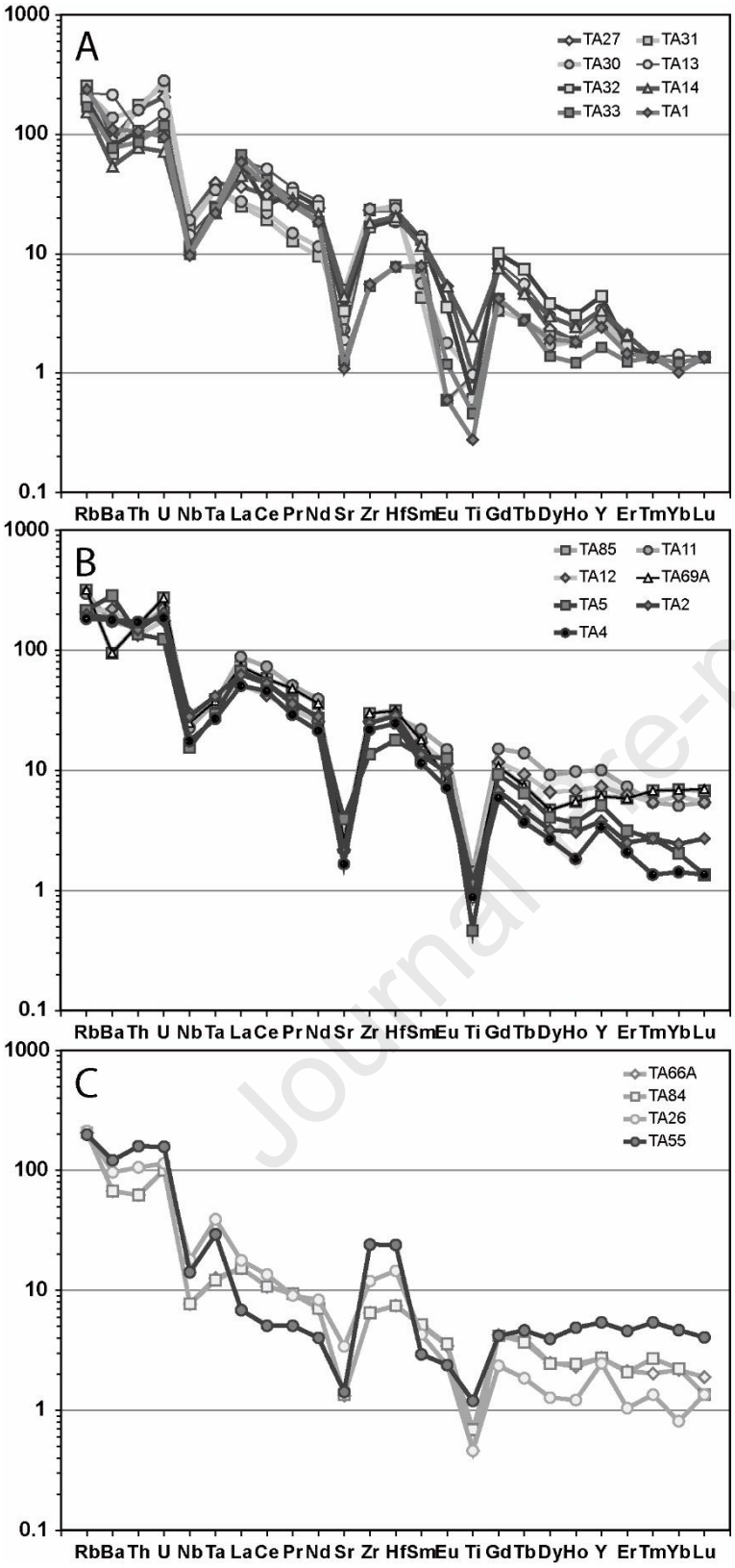

Figure 9: Primitive Mantle normalized multi-element diagram of volcanic rocks from the Tagragra-n-Daouizid area. **A.** Group 1 rhyolites; **B.** Groups 2 and 3 rhyolites; **C.** Group 4 rhyolites. Normalization according to Sun and McDonough, 1989.

4.3. Tagragra Ouhallal area

LOI of basaltic trachy-andesites and trachy-andesites are high, however we did not observe signicative correlation between LOI and an excess or a loss in alkali elements. The compositions are representative of the original magma. Major elements variations are illustrated in Figure 4 using silica variations diagrams. These lavas have intermediate compositions (SiO_2=52.7-59.1 wt%), with high Al_2O_3 (16-21 wt%), intermediate to high Fe_2O_3 (6.2-8.6 wt%) and K_2O contents (2.7-5.3 wt%), low to intermediate MgO (1.7-5.6 wt%), and Na_2O (1.8-5.7 wt%), and low CaO contents (0.9-3.5 wt%). These rocks are alkaline and Ti-rich (0.75-1.47 wt%), with magnesian affinities (Fig. 7).

Basaltic trachyandesites and trachyandesites display REE patterns characterized by fractionated LREE ($1.4<[La/Sm]_n<7.6$) and highly fractionated HREE ($5.0<[Gd/Yb]_n<11.0$) without negative Eu anomalies. HREE are lower than ten times chondrites ($[Yb]_n$=1.8-4.7; Fig. 5C). In the Primitive Mantle normalizing diagram (Fig. 6C), patterns do not display systematic negative anomalies in Ta and Nb.

Rhyolites display major element compositions typical of potassic to high-potassic rhyolites with SiO_2 contents ranging between 71.8 to 85.3 wt%, and alkali concentrations control essentially by K_2O contents (2.6-4.7 wt%; Fig. 4).

5. Discussion

5.1. Summary of the depositional environment

In the Tafeltast area, the Ouarzazate Group is essentially composed of terrigenous sediments with few volcano-sedimentary rocks and pyroclastic deposits. These sedimentary deposits are located in narrow grabens controlled by syn-sedimentary normal faults, and were formed in fluvial-lacustrine system. This lacustrine sedimentation is characterized by a maximum flooding outlined by the development of a carbonate key bed, the Agoujgal carbonates.

In the Tagragra-n-Daouizid area, the Ouarzazate Group represents the surficial emission of a rhyolitic magma in pyroclastic flows. Effusive flows or domes are missing. This pyroclastic eruptive activity, probably very brief in time, was closely associated with continental sedimentary deposits, mostly coarse brecciated or conglomeratic.

In the Tagragra Ouahallal area, the massive ash layers at the base of the sequence, the intrusive pillow lavas in waterlogged deposits, the stacking of lava flows, the geographical distribution of the flows on

one side and of the pillow lavas on the other side, the frequent alternation of emerged and submerged periods under shallow water, are quite comparable to that described in subglacial mafic volcanoes (Smellie and Skilling, 1994; Skilling, 1994); However, such a depositional environment is not observed in the other areas where the depositional system is almost systematically fluvial-lacustrine.

In the neighboring Kerdous inlier, Upper Ediacaran rocks are essentially volcaniclastic rocks and rhyolitic lavas and domes (O'Connor, 2010). Upper Ediacaran sedimentary, volcaniclastic and volcanic rocks have been divided in three main groups: i) Oufoud; ii) Tanalt; and iii) Fiyzirt (O'Connor, 2010). On the southern border of the Kerdous inlier, the Oufoud Group, characterized by a dominantly conglomeratic sequence with rhyodacitic lava and ignimbrite. In the centre of the Kerdous inlier, the Tanalt Group comprises a succession of matrix-supported conglomerate, coarse-grained to well-bedded fine sandstone and siltstone, with locally interbedded rhyolitic welded pyroclastic tuff. On the eastern border of the Kerdous inlier, the Fiyzirt Group comprises conglomerate, sandstone, basaltic lava and shallow level intrusion. Lavas and tuffs were emplaced throughrout the sedimentary rocks which were deposited in a subaerial environment, probably on alluvial fan and flood plains with local shallow lakes (O'Connor, 2010). Geochemically, volcanic rocks have high-K calc-alkaline to alkaline affinities, characteristics of both subduction and within-plate tectonic settings (O'Connor, 2010).

In the Bas Draâ inlier, the volcanic activity evolved in a continental extensional setting (Karaoui et al., 2014). The Ouarzazate Group is characterized by four distinct units (Karaoui et al., 2014): i) rhyolitic ignimbrite; ii) rhyolitic lava-dome and basaltic andesite scoria cone, with rare ignimbrite; iii) basaltic to basaltic andesite lavas with minor pyroclastic deposits; and iv) rhyolitic lava-dome. Sedimentary processes are characteristics of fluvial systems, and the lack of volcanosedimentary mass flow deposits indicates a low relief environment (Karaoui et al., 2014). Geochemically, volcanic rocks have high-K calc-alkaline, alkali-calcic and alkaline affinities, characteristics of both subduction and within-plate tectonic settings (Karaoui et al., 2014).

5.2. Tectonic discrimination diagrams

Geochemical data of the mafic to intermediate lavas from the Kerdous inlier and the Tagragra Ouhallal area provide important informations regarding their tectonic setting. On the Y/15–La/10–Nb/8 diagram (Fig. 10), mafic lavas from the Kerdous inlier and the Tagragra Ouhallal area fall in the calc-alkaline basalt and continental tholeiite fields. Like these lavas, basalts from the Bas Draâ (Karaoui et al., 2014)

and Agadir-Melloul (Blein et al., 2014b) inliers fall in the fields of calc-alkaline basalts and continental tholeiites. Basalts from the southwestern or northeastern flank of the Kerdous inlier (Soulaimani et al., 2004) fall on the boundary between the fields of the continental tholeiites and back-arc basalts. These Upper Ediacaran basalts are distinguished from the Cambrian basalts of the jbel Boho (Bou Azer inlier; Benaouda et al., 2017) which have an affinity of alkaline basalts to continental tholeiites. The Upper Ediacaran mafic rocks show a clear south-north evolution from continental tholeiites to back-arc basalts, characterized by a relative enrichment in Y compared to La and Nb. This volcanic activity occurred during an extensional episode, certainly more important in the north than in the south because the mantle source has a more asthenospheric signature in the north than in the south.

As shown in Figure 11 (FeO^t+MgO versus Nb+Zr+Y, La_n and Sr+Ba), intermediate to felsic rocks can be classified into two main groups: i) low FeO^t+MgO (<7 wt.%) metaluminous to peraluminous rocks, with moderate incompatible element contents, generated mainly by partial melting of crustal lithologies; and ii) high FeO^t+MgO (>7 wt.%) metaluminous intermediate to felsic rocks with moderate incompatible element contents, generated by an enriched mantle source with variable involvement of crustal component.

Whalen and Hildebrand (2019) developed new diagrams to discriminate between arc, slab-failure and A-type granitoids. These diagrams are valid for non peraluminous samples (ASI < 1.1), with SiO_2 concentrations ranging between 55 and 70 wt%. Samples from the Ouarzazate Group that meet these criteria have been plotted in such diagrams (Fig. 12A-B).

With high Nb/Y, Gd/Yb, and La/Yb ratios, samples from Tagragra Ouhallal plot in the slab-failure field, while samples from the Kerdous and Agadir-Melloul inliers, with lower Nb/Y, La/Yb and Gd/Yb ratios and plot at the limit between arc and slab-failure fields (Fig. 12A-B). As typical characteristic of magmas generated by slab-failure, samples from Tagragra Ouhallal have low Ta+Yb values (Fig. 12B). All samples have Ta/Yb ratios higher than 0.3., and plot in the field of slab-failure magmas (Fig. 12B). Their high La/Yb (>10), and Nb/Y (>0.4) ratios are typical of slab-failure rocks (Fig. 12A-B). Samples from the Kerdous and Agadir-Melloul inliers, and the Tagragra-n-Daouizid area, with higher Ta+Yb values, and lower La/Yb, and Nb/Y ratios than samples from the Tagragra Ouhallal area. In Figure 12A-B, they plot at the limit between arc and slab-failure fields.

On Y vs. Nb and Yb vs. Ta diagrams (Fig. 12C-D), the samples from the Tagragra Ouhallal and Tagragra-n-Daouizid areas also plot in the slab-failure field, while samples from the Kerdous inlier plot

close to the triple point between arc, slab-failure and A-type fields, which is characteristic of granites formed in post-collisional extensional settings (Förster et al., 1997).

Geochemical data indicate that: (i) mafic rocks are essentially continental flood basalt; (ii) felsic rocks are high-K calc-alkaline rocks, generated by partial melting of an enriched mantle source with involvement of crustal component; and (iii) few intermediate and felsic rocks sharing characteristics with slab failure magma (Hildebrand and Whalen, 2017).

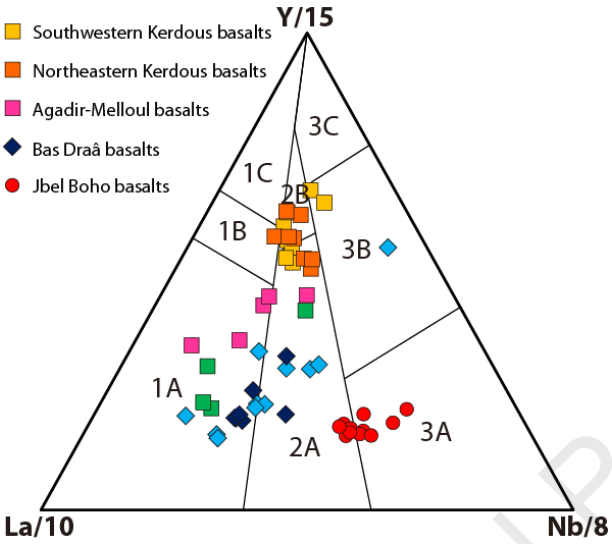

Figure 10: Y/15–La/10–Nb/8 diagram (Cabanis and Lecolle, 1989) for mafic rocks (SiO_2 < 55 wt%) of the Ouarzazate Group (1A: Calc-alkaline basalts; 1B: Calc-alkaline basalts and arc tholeiites; 1C: Volcanic arc tholeiites; 2A: Continental tholeiites; 2B: Back-arc basalts; 3A: Alkaline basalts; 3B: E-type MORB; 3C: N-type MORB; Symbols as in Fig. 3).

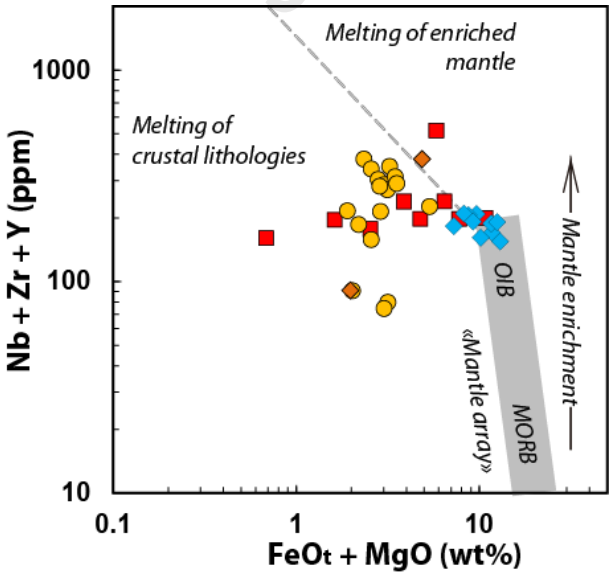

Figure 11: (FeO^t+MgO) vs. (Nb=Zr+Y) diagram (Symbols as in Fig. 3).

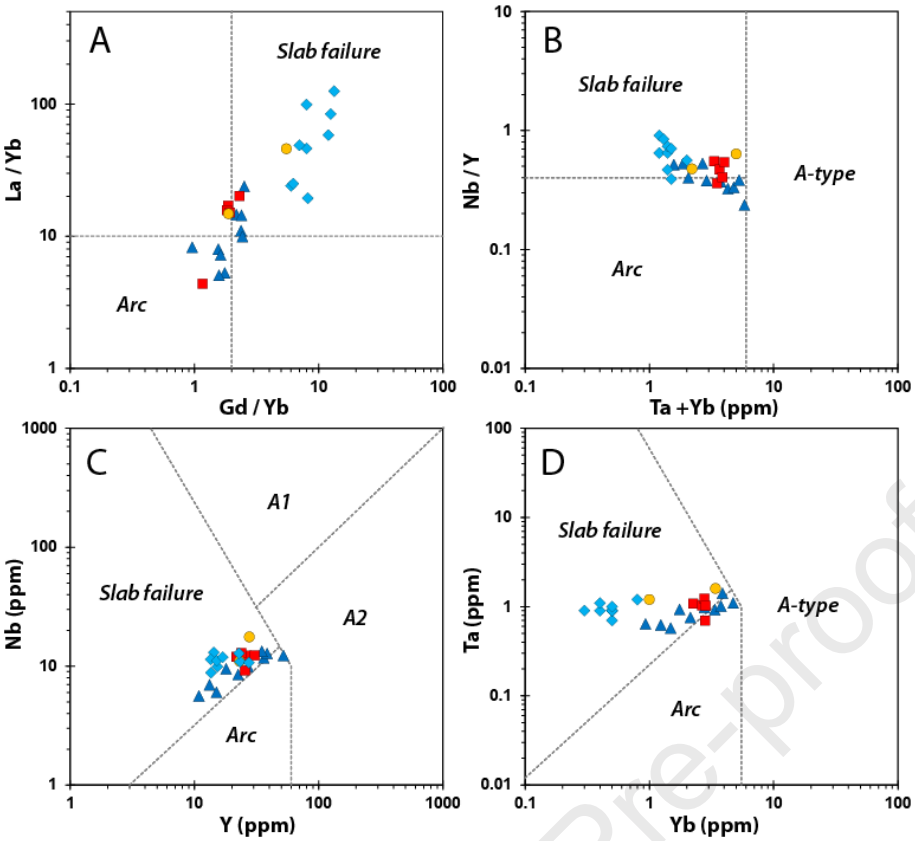

Figure 12: Discrimination diagrams showing slab failure, A-type and arc fields (Hildebrand and Whalen, 2014; Hildebrand et al., 2018; Whalen and Hildebrand, 2019). Samples, plotted on diagrams, have SiO_2 contents between 55 and 70 wt%, and alumina saturation index (ASI) value lower than 1.1: **A.** Gd/Yb vs La/Yb; **B.** Ta+Yb vs. Nb/Y; **C.** Y vs. Nb; and **D.** Yb vs. Ta. Symbols as in Fig. 3. Light blue triangle: Ouarzazate Group from the Agadir Melloul inlier (Blein et al., 2014b).

5.3. Geodynamic setting

Thomas et al. (2004) divided the Neoproterozoic igneous rocks of the Anti-Atlas belt in two main supergroups: Anti-Atlas and Ouarzazate supergroups. The lithostratigraphic units of the Anti-Atlas Supergroup are related to passive margin, oceanic and island-arc development phases of the Pan African orogen before ca. 650 Ma. All the younger plutonic, volcanic and sedimentary rocks have been grouped into the Ouarzazate Supergroup. The pre 580 Ma volcano-sedimentary rocks of the Ouarzazate Supergroup were deposited in narrow strike-slip pull-apart basins (Saghro, Bou Salda, Mgouna, Tafrawt and Anzi groups) contemporaneously with high-K calc-alkaline plutons (e.g., Assarag, Bardouz Suites). These rocks were followed by the uncomformable continental deposition of voluminous pyroclastic deposits and volcano-sedimentary rocks (the Ouarzazate Group); the volcanic rocks were erupted from several volcanic centers and caldera complexes, and are younger than 580 Ma (Thomas et al., 2002;

El Baghdadi et al., 2003; Gasquet et al., 2005, 2008; Errami et al., 2009; Toummite et al., 2012; Walsh et al., 2012; Blein et al., 2014b; Baidada et al., 2017; Belkacim et al., 2017).

Set up between ca. 575 and ca. 545 Ma, the Ouarzazate Group can be subdivided into three major magmatic pulses dated between: (i) 575 and 570 Ma, (ii) 568 and 563 Ma, (iii) and 555 and 545 Ma. In the Agadir-Melloul inlier, Blein et al. (2014b) highlighted angular unconformities between each volcanic pulses. The first unconformity is placed around ca. 568 Ma and the younger at ca. 560 Ma. The latter angular unconformity has been described in the Saghro massif (Walsh et al., 2012), and in the western Anti-Atlas (Blein et al., 2014b). Finally, the last one is in continuity with the sedimentary rocks of the Adoudou Formation. A complete stratigraphy of these three pulses has been observed in the Agadir-Melloul inlier (Blein et al., 2014b) and in the Saghro massif (Errami et al., 2020; Yajioui et al., 2020).

In the Saghro massif, before the deposition of the Ouarzazate Group, Imiter and Iknioun granodiorites (600–603 Ma) were uplifted and exhumed. The Oussilkane charnockite, dated at 580±19 Ma (Errami et al., 2020), is contemporaneous with this phase of uplift. In the Bou Azer inlier, the ignimbrites of the Ouarzazate Group were deposited unconformably on the volcano-sedimentary sequence of the Tiddiline Group (602–606 Ma), and on the uplifted and exhumed Bleïda granodiorite (579±2 Ma; Inglis et al., 2004). These observations suggest the occurrence of an uplift between ca. 580 and ca. 575 Ma.

Late Ediacaran geodynamic models are the subject of much debate. A scenario suggest the occurrence of a subduction ca. 625–560 Ma to explain the Ouarzazate high-K calc-alkaline magmatism (El Baghdadi et al.,2003; Benziane, 2007; Walsh et al., 2012; Hefferan et al., 2014). Another scenario suggest a post-collisional transtensional setting, without subduction, for the late Ediacaran Pan-African orogeny (Doblas et al., 2002; Thomas et al., 2002; Gasquet et al., 2005; Karaoui et al., 2015). Blein et al. (2014b) propose a subduction beneath the WAC ca. 625–580 Ma, followed by the arrival of a spreading ridge at the subduction zone at ca. 580–575 Ma, and post ca. 575 Ma by the pyroclastic magmatism in a transtensive setting (Ouarzazate Group).

Tuduri et al. (2018) put forward a closer model with the development of a subduction between 610 and 575 Ma, followed by the initiation of a slab roll-back around ca. 575 Ma. This slab roll-back resuts in large volume of magma, leading to the pyroclastic flows of the Ouarzazate Group. And ongoing slab roll-back along with more extensional tectonic setting initiate the second, and then the third ignimbritic pulses (Tuduri et al., 2018).

Dominated by the eruptions of thousands of cubic kilometers of pyroclastic flows, volcanic activity of the Ouarzazate Group is typical of ignimbrite flare-ups. Originally, flare-ups are short-lived large volumes of silicic ignimbrites in orogenic setting, inland from the plate margin (Lipman et al., 1971; Noble, 1972). These flare-ups are intercalated in the stable magmatism of an active margin, characterized by andesitic volcanic and intrusive rocks. This stable active margin magmatism is characterized by low magmatic addition rates (MAR). Flare-ups are typically short-time high-MAR episodes, alternating with longest low-MAR episodes.

High-resolution zircon geochronological ages reveal multiple events and the intermittent nature of flare-ups at various scales of space, time, and volumes (Folkes et al. 2011; Lima et al. 2012; Silva et al., 2015). Considered as a primary pulse, the flare-up or high-volume event is a 40-50 my mantle activity induced by: (i) post-collisional mantle delamination (Ducea, 2001), (ii) a regional transition from low-angle to high-angle plate convergence in relation to slab roll-back (Lipman et al., 1972; Best et al., 2013), or (iii) slab breakoff (Ferrari et al., 2002). This primary pulse can be broken down in secondary pulses. These shorter secondary pulses (~10–20 my) must reflect the timescale of melt production and delivery from the melting and assimilation zone, and its interaction with the upper crust (de Silva et al., 2015). Typically observed in Andean volcano-plutonic systems, such 10 my secondary pulses are an essential signal in orogenic magmatic activity (Coleman et al., 2004; Grunder et al., 2008). Due to its duration (~30–35 my), the pyroclastic volcanism of the Ouarzazate Group is a typical primary pulse, the three ignimbritic pulses observed in Agadir Melloul (Adrar-n-Takoucht, Tadoughast and Fajjoud formations) and Imiter (~10 my in duration) are typically secondary pulses.

According to DeCelles et al. (2009), flare-ups are periods of high rates of magma production, relative to the normal state rates of arc-magma production. A transition from low-angle to high-angle plate convergence in relation to slab roll-back may explain such higher magmatic fluxes, and episodic alternations between magmatic lulls and flare ups (Ferrari et al., 2007). In the Anti-Atlas, the late Ediacaran magmatic activity is not characterized by episodic alternations between normal arc-magma production and flare up activity, but by an individual flare up event predating the development of a Cambrian marine carbonate platform (Alvaro et al., 2014). There are many mechanisms to explain such individual flare up events such as: (i) slab break-off (e.g., Schwartz et al., 2017), (ii) subduction of fracture zones (e.g., Manea et al., 2014), or (iii) subduction of continental lithospheric mantle before a collision (e.g., Ganade et al., 2021). In our case, the late Ediacaran flare up event is related to a slab

588 break-off event. As the late Ediacaran Ouarzazate magmatism is not followed by a continental collision
589 event, it cannot be related to the subduction of continental lithospheric mantle, and the late Ediacaran
590 flare up event is widespread, and not geographically restricted like in subduction of fracture zones.
591 Moreover, volcanic rocks of the Ouarzazate Group fall in the field of slab-failure rocks (Fig. 11).

592 6. Conclusions

593 New constraints on the late Ediacaran evolution of the western Anti-Atlas New have been provided from
594 geological mapping, petrography and geochemistry of volcano-sedimentary rocks of the southern
595 Kerdous and Tagragra d'Akka inliers.

596 In the Kerdous and Tagragra d'Akka inliers, the Ouarzazate Group consists of terrigenous sediments,
597 volcano-sedimentary rocks, basaltic flows and dacitic to rhyolitic, welded or unwelded, pyroclastic tuffs.
598 These deposits are located in grabens controlled by syn-sedimentary normal faults. The sedimentation
599 is characterized by a maximum flooding outlined by the Agoujgal carbonates. Dacitic to rhyolitic
600 pyroclastic tuffs of the Ouarzazate Group have a high-potassic calc-alkaline affinity. Basalts observed
601 in the Kerdous inlier and the Tagragra Ouahallal area have transitional affinity between continental
602 tholeiites and calc-alkaline basalts. Few intermediate and felsic volcanic rocks are characteristics of slab
603 failure rocks derived from melting of mafic upper portion of the subducted slab (Hildebrand and Whalen,
604 2017).

605 The Ouarzazate flare up event is related to the cessation of a subduction, which induced a slab break-
606 off. The late Ediacaran Ouarzazate magmatism in not followed by a continental collision event, and
607 cannot be related to the subduction of continental mantle lithosphere; the late Ediacaran flare up event
608 is widespread, and not geographically restricted like in subduction of fracture zones.
609

Credit authorship contribution statement

Olivier Blein: Interpretation of chemical data and wrote the manuscript. Thierry Baudin, Philippe Chèvremont, and Dominique Gasquet: Contributed in the field work, sampling, and to the writing of the manuscript.

Declaration of competing interest

The authors declare that they have no known competing financial interests or personal relationships that could have appeared to influence the work reported in this paper.

Acknowledgements

Funding was provided by the Moroccan Ministry of Energy, Mines, Water and Environment (contracts 19-2008/DG) with the production of geological four mapsheets and explanatory notes (Sidi Bou'Addi, Awkarda, Tamazrar, Tlatat Ida Gougmar).

References

Abati, J., Aghzer, A.M., Gerdes, A., Ennih, N., 2010. Detrital zircon ages of Neoproterozoic sequences of the Moroccan Anti-Atlas belt. Precambrian Research 181, 115–128. https://doi:10.1016/j.precamres.2010.05.018.

Aït Lahna, A., Youbi, N., Tassinari, C.C.G., Basei, M.A.S., Ernst, R.E., Chaib, L., Barzouk, A., Mata, J., Gärtner, A., Admou, H., Boumehdi, M.A., Söderlund, U., Bensalah, M.K., Bodinier, J.L., Maacha, L., Bekker, A., 2020. Revised stratigraphic framework for the lower Anti-Atlas supergroup based on U-Pb geochronology of magmatic and detrital zircons (Zenaga and Bou Azzer-El Graara inliers, Anti-Atlas Belt, Morocco), J. Afr. Earth Sci. 171, 103946. https://doi:10.1016/j.jafrearsci.2020.103946.

Aït Malek, H., Gasquet, D., Bertrand, J. M., Leterrier J., 1998. Géochronologie U-Pb sur les granitoïdes éburnéens et panafricains dans les boutonnières protérozoïques d'Igherm, du Kerdous et du Bas Drâa (Anti-Atlas occidental, Maroc). Comptes Rendus de l'Académie des Sciences 327, 819–826. https://doi:10.1016/S1251-8050(99)80056-1.

635 Alvaro, J.J., Clausen, S., El Albani, A., Chellai, E.H., 2005. Facies distribution of Lower Cambrian
636 cryptic microbial and epibenthic archaeocyathan–microbial communities in the western Anti-Atlas,
637 Morocco. Sedimentology, 53, 35–53. https://doi:10.1111/j.1365-3091.2005.00752.x.
638 Álvaro, J.J., Bellido, F., Gasquet, D., Francisco Pereira, M., Quesada, C., Sánchez-García, T., 2014.
639 Diachronism in the late Neoproterozoic–Cambrian arc-rift transition of North Gondwana: A
640 comparison of Morocco and the Iberian Ossa-Morena Zone. Journal of African Earth Sciences 98:
641 113–132.
642 Baidada, B., Cousens, B., Alansari, A., Soulaimani, A., Barbey, P., Ilmen, S., Ikenne, M., 2017.
643 Geochemistry and Sm-Nd isotopic composition of the Imiter Pan-African granitoids (Saghro massif,
644 eastern Anti-Atlas, Morocco): Geotectonic implications. J. Afr. Earth Sci. 127, 99–112.
645 https://doi:10.1016/j.jafrearsci.2016.08.016.
646 Bajja, A., 1998. Volcanisme syn à post-orogénique du Néoprotérozoïque de l'Anti-Atlas: implications
647 pétrographiques et géodynamiques (Thèse de doctorat d'Etat). Université Chouaib Doukkali, El
648 Jadida, Maroc (215 p.).
649 Bajja, A., 2001. Volcanisme syn a post orogénique du Néoprotérozoïque de l'Anti-Atlas: implications
650 pétrogénétiques et géodynamiques. In: De Wall, H., Greiling, R.P. (Eds.), Magmatic Evolution of a
651 Neoproterozoic island-Arc syn-to Post-orogenic Igneous Activity in the Anti-Atlas (Morocco),
652 Forschunszentrum Jülich Gmbh, vol. 45, pp. 9–228.
653 Baudin, T., Razin, P., Chèvremont, P., Calvès, G., Gabudianu, D., Roger, J., 2005. Carte géol. Maroc
654 (1/50 000), feuille Awkarda. Notes et Mémoires Serv. Géol., Maroc, n°497.
655 Belkacim, S., Gasquet, D., Liégeois, J.P., Arai, S., Ghalan, H., Ahmed, H.A., Ishida, Y., Ikenne, M.,
656 2017. The Ediacaran volcanic rocks and associated mafic dykes of the Ouarzazate Group (Anti-
657 Atlas, Morocco): Clinopyroxene composition, whole-rock geochemistry and Sr-Nd isotopes
658 constraints from the Ouzellarh-Sirwa salient (Tifnoute valley). J. Afr. Earth Sci. 127, 113–135.
659 https://doi:10.1016/j.jafrearsci.2016.08.002
660 Benaouda, R., Holzheid, A., Schenk, V., Badra, L., Ennaciri, A., 2017. Magmatic evolution of the Jbel
661 Boho alkaine complex in the Bou Azzer inlier (Anti-Atlas, Morocco) and its relation to REE
662 mineralization. J. Afr. Earth Sci. 129; 202–223. https://doi:10.1016/j.jafrearsci.2017.01.003.

663 Benssaou, M., Hamoumi, N. 2001. L'Anti-Atlas occidental du Maroc: étude sédimentologique et
664 reconstitutions paléogéographiques au Cambrien inférieur. J. Afr. Earth Sci. 32, 351–372.
665 https://doi:10.1016/S0899-5362(01)90102-2
666 Benssaou, M., Hamoumi, N. 2003. Le graben de l'Anti-Atlas occidental (Maroc) : contrôle tectonique
667 de la paléogéographie et des séquences du Cambrien inférieur. C.R. Géoscience 335, 297–305.
668 https://doi:10.1016/S1631-0713(03)00033-6
669 Benziane, F., 2007. Lithostratigraphie et évolution géodynamique de l'Anti-Atlas (Maroc) du
670 Paléoprotérozoïque au Néoprotérozoïque: exemples de la boutonnière de Tagragra de Tata et du
671 Jbel Saghro. PhD thesis. Université de Savoie CISM, Chambéry, France, 320 pp.
672 Best, M.G., Christiansen, E.H., Gromme, S., 2013. Introduction: the 36–18 Ma southern Great Basin,
673 USA, ignimbrite province and flare up: swarms of subduction-related supervolcanoes. Geosphere
674 9: 260–274.
675 BGS, 2001a. Carte géologique du Had-n-Tahala au 1/50 000. Notes et Mémoires, 403, Editions du
676 Service Géologique du Maroc, Rabat.
677 BGS, 2001b. Carte géologique d'Anzi au 1/50 000. Notes et Mémoires, 402, Editions du Service
678 Géologiques du Maroc, Rabat.
679 Blein, O., Chèvremont, Ph., Baudin, T., Ouanaimi, H., Razin, Ph., Hafid, A., Admou, H., Soulaimani,
680 A., Bouabdelli, M, Abia, E.H., Beni Akhy, R., 2013. Notice explicative carte géol. Maroc (1/50 000),
681 feuille Tabadrist, Notes et Mémoires Serv. Géol. Maroc, n°547, MEM/BRGM. Carte géologique par
682 Baudin, T., Blein, O., Chèvremont, Ph., Soulaimani, A., Ouanaimi, H., Roger, J., Admou, H., Hafid,
683 A., Bouabdelli, M., Abia, E.H., 2013.
684 Blein, O., Baudin, T., Chèvremont, P., Soulaimani, A., Admou, H., Gasquet, D., Cocherie, A., Egal, E.,
685 Youbi, N., Razin, P., Bouabdelli, M., Gombert, Ph., 2014a. Geochronological constraints on the
686 polycyclic magmatism in the Bou Azzer-El Graara inlier (Central Anti-Atlas Morocco). J. Afr. Earth
687 Sci. 99, 287–306. https://doi:10.1016/j.jafrearsci.2014.04.021.
688 Blein, O., Baudin, T., Soulaimani, A., Cocherie, A., Chèvremont, P., Admou, H., Ouanaimi, H., Hafid,
689 A., Razin, P., Bouabdelli, M., Roger, J., 2014b. New Geochemical, Geochronological and Structural
690 Constraints on the Ediacaran Evolution of the South Sirwa, Agadir Melloul and Iguerda Inliers, Anti-
691 Atlas, Morocco. J. Afr. Earth Sci. 98, 47–71. https://doi.org/10.1016/j.jafrearsci.2014.06.019

692 Blein, O., Chèvremont, P., Baudin, T., Hafid, A., Admou, H., Soulaimani, A., Ouanaimi, H., Bouabdelli,
693 M., Gasquet, D., Padel, M., 2022. Contrasting Paleoproterozoic granitoids in the Kerdous,
694 Tragragrad'Akka, Agadir-Melloul and Iguerda inliers (western Anti-Atlas, Morocco). J. Afr. Earth
695 Sci. 189, 104500. https://doi.org/10.1016/j.jafrearsci.2022.104500
696 Boudda, A., Choubert, G., Faure-Muret, A., 1979. Essai de stratigraphie de la couverture sédimentaire
697 de l'Anti-Atlas : Adoudounien-Cambrien inférieur. Notes et Mémoires du Service Géologique du
698 Maroc 271, 96 p.
699 Bouougri, E.H., Saquaque, A., 2004. Lithostratigraphic framework and correaltion of the
700 Neoproterozoic northern West African Craton passive margin sequence (Siroua – Zenaga - Bou
701 Azzer El Graara inliers, central Anti-Atlas, Morocco): an integrated approach. J. Afr. Earth Sci. 99,
702 287–306. https://doi:10.1016/j.jafrearsci.2004.07.045.
703 Cabanis, B., Lecolle, M., 1989. Le diagramme La/10-Y/15-Nb/8 : un outil pour la discrimination des
704 séries volcaniques et la mise en évidence des processus de mélange et/ou de contamination
705 crustale. C. R. Acad. Sci. Ser. II 309, 2023–2029.
706 Carignan, J., Hild, P., Mévelle, G., Morel, J., Yeghicheyan, D., 2001. Routine analyses of trace
707 elements in geological samples using flow injection and low pressure on-line liquid chromatography
708 coupled to ICP-MS: a study of reference materials BR, DR-N, UB-N, AN-G and GH. Geostandards
709 Newsl. 25, 187–198.
710 Chalot-Prat, F., Gasquet, D., Roger, J., Hassenforder, B., Chèvremont, P., Baudin, T., Razin, P.,
711 Benlakhdim, A., Benssaou, M., Mortaji, A., 2001. Carte géologique du Maroc au 1/50000. Feuille
712 de Sidi Bou'Addi avec Mémoire explicatif. Notes et Mémoires du Service Géologique du Maroc 414
713 & 414 bis, 84 p.
714 Cheilletz, A., Levresse, G., Gasquet, D., Azizi Samir, M.R., Zyadi, R., Archibald, D.A., 2002. The Imiter
715 epithermal deposit (Morocco): new petrographic, microtectonic and geochronological data.
716 Importance of the Precambrian–Cambrian transition for major precious metals deposits in the Anti-
717 Atlas. Miner. Deposita 37, 772–781.
718 Chèvremont, P., Razin, P., Baudin, T., Gabudianu, D., Roger, J., Thiéblemont, D., Calvès, G., Anzar-
719 Conseil, 2005. Notice explicative, carte géol. Maroc (1/50 000), feuille Awkarda, Notes et Mém.
720 Serv. Géol. Maroc, n°497bis, MEM/BRGM, 114 p. Carte géol. par Baudin T., Razin P., Chèvremont
721 P., Calvès G., Gabudianu D., Roger J. (2005), Notes et Mém. Serv. Géol. Maroc, n°497.

Chèvremont, P., Blein, O., Razin, P., Simon, B., Baudin, T., Ouanaïmi, H., Soulaimani, A., El Janati, M., Bouabdelli, M., Abia, E.H., Admou, H., Hafid, A., Beni Akhy, R., 2013. Notice explicative carte géol. Maroc (1/50 000), feuille Ighriy, Notes et Mémoires Serv. Géol. Maroc, n°548, MEM/BRGM. Carte géologique par Ouanaimi, H., Chèvremont, Ph., Blein, O., Simon, B., Baudin, T., Razin, Ph., Smektala, F., Soulaimani, A., El Janati, M., Abia, E.H., Admou, H., Hafid, A., Bouabdelli, M., 2013.

Choubert, G., 1952. Histoire géologique du domaine de l'Anti-Atlas. In: Géologie du Maroc. Notes et Mémoires du Service Géologique du Maroc 100, 75–194.

Choubert, G., 1953a. Histoire géologique du domaine de l'Anti-Atlas. Notes et Mémoire de Service géologique du Maroc 100, 1–77.

Choubert, G., 1953b. Le Précambrien III et le Géorgien de l'Anti-Atlas. Notes et Mémoire de Service géologique du Maroc 103, 7–39.

Choubert, G., 1963. Histoire géologique du Précambrien de l'Anti-Atlas. Notes et Mémoires du Service Géologique du Maroc 162, 443 p.

Choubert, G., Faure-Muret, A., 1970. Colloque international sur les corrélations du Précambrien, Agadir-Rabat, 3–23 mai 1970, et livret-guide de l'excursion: Anti-Atlas occidental et central, Notes Mém. Serv. Géol. Maroc 229, 259p.

Choubert, G., Boudda, A., Faure-Muret, A., 1973. Essai de Chronologie du Précambrien supérieur du sud marocain: C. R. Somm. S.G.F, 123–124.

Clauer, N., 1976. Géochimie isotopique du Strontium des milieux sédimentaires. Application à la géochronologie de la couverture du Craton Ouest-Africain. Strasbourg.

Coleman, D.S., Glazner, A.F., 1997. The Sierra Crest magmatic event: rapid formation of juvenile crust during the Late Cretaceous in California. International Geology Review 39: 768–787.

DeCelles, P.G., Ducea, M.N., Kapp, P., Zandt, G., 2009. Cyclicity in Cordilleran orogenic systems. Nature Geoscience 2: 251–257

De Silva, S.L., Riggs, N.R., Barth, A.P., 2015. Quickening the pulse: Fractal tempos in continental arc magmatism. Elements 11, 113–118. https://doi:10.2113/gselements.11.2.113.

D'Lemos, R.S., Inglis, J.D., Samson, S.D., 2006. A newly discovered orogenic event in Morocco: Neoproterozoic ages for supposed Eburnean basement of the Bou Azzer inlier, Anti-Atlas Mountains. Precambrian Research 147, 65–78.

751 Doblas, M., Lopez-Ruiz, J., Cebria, J.M., Youbi, N., Degroote, E., 2002. Mantle insulation beneath the
752 west African craton during the Precambrian–Cambrian transition. Geology 30, 839–842.
753 Ducea, M., 2001. The California arc: thick granitic batholiths, eclogitic residues, lithospheric-scale
754 thrusting, and magmatic flare-ups. GSA Today 11, 4–10.
755 Ducrot, J., Lancelot, J.R., 1977. Problème de la limite Précambrien-Cambrien : étude radio-
756 chronologique par la méthode U-Pb sur zircons du volcan du Jbel Boho (Anti-Atlas Marocain).
757 Canadian Journal of Earth Sciences 14, 2771–2777.
758 Eddif, A., Gasquet, D., Hoepffner, C., Levresse, G., 2007. Age of the Wirgane granodiorite intrusions
759 (Western High Atlas, Morocco): new U–Pb constraints. J. Afr. Earth Sci. 47, 227–231.
760 El Baghdadi, M., El Boukhari, A., Jouider, A., Benyoucef, A., Nadem, S., 2003. Calc-alkaline arc I-type
761 granitoid associated with S-type granite in the Pan-African belt of eastern Anti-Atlas (Saghro and
762 Ougnat, South Morocco). Gondwana Res. 6 (4), 557–572. https://doi:10.1016/S1342-
763 937X(05)71007-8.
764 Ennih, N., Liégeois, J.-P., 2008. The boundaries of the West African Craton, with special reference to
765 the basement of the Moroccan metacratonic Anti-Atlas belt. Geological Society, London, Special
766 Publications 297 (1), 1–17. https://doi:10.1144/SP297.1.
767 Errami, E., Bonin, B., Laduron, D., Lasri, L., 2009. Petrology and geodynamic significance of the post-
768 collisional Pan-African magmatism in the Eastern Saghro area (Anti-Atlas, Morocco). J. Afr. Earth
769 Sci. 55, 105–124. https://doi:10.1016/j.jafrearsci.2009.02.006.
770 Errami, E., Linnemann, U., Hofmann, M., Gärtner, A., Zieger, J., Gärtner, J., Mende, K., El Kabouri, J.,
771 Gasquet, D., Ennih, N., 2020. From Pan-African Transpression to Cadomian Transtension at the
772 West African Margin: New U–Pb zircon Ages from the Eastern Saghro Inlier (Anti-Atlas, Morocco).
773 *In* Murphy, J. B., Strachan, R. A. and Quesada, C. (eds). Pannotia to Pangaea: Neoproterozoic and
774 Paleozoic Orogenic Cycles in the Circum-Atlantic Region. Geological Society, London, Special
775 Publications, 503. https://doi:10.1144/SP503-2020-105.
776 Fekkak, A., Pouclet, A., Ouguir, H., Badra, L., and Gasquet, D., 1999, The Kelaat Mgouna early
777 Neoproterozoic Group (Saghro, Anti-Atlas, Morocco): Witness of an initial stage of the pre-Pan-
778 African extension: Bulletin de la Société Géologique de France, 170, 789–797.

779 Fekkak, A., Boualoul, M., Badra, L., Amenzou, M., Saquaque, A., El-Amrani, I. E., 2000. Origine et
780 contexte géotectonique des dépôts détritiques du Groupe Néoprotérozoïque inférieur de Kelaat
781 Mgouna (Anti-Atlas Oriental, Maroc). Journal of African Earth Sciences 30, 295–311.
782 Fekkak, A., Pouclet, A., Benharref, M., 2003. The Middle Neoproterozoic Sidi Flah Group (Anti-Atlas,
783 Morocco): synrift deposition in a Pan-African continent/ocean transition zone. J. Afr. Earth Sci. 37,
784 73–87. https://doi:10.1016/S0899-5362(03)00049-6.
785 Ferrari, L., Lopez-Martinez, M., Rosas-Elguera, J., 2002. Ignimbrite flare-up and deformation in the
786 southern Sierra Madre Occidental, western Mexico: Implications for the late subduction history of
787 the Farallon plate. Tectonics 21 (4). https://doi:10.1029/2001TC001302.
788 Ferrari L, Valencia-Moreno M, Bryan S (2007) Magmatism and tectonics of the Sierra Madre
789 Occidental and its relation with the evolution of the western margin of North America. Geological
790 Society of America Special Paper 422: 1-39.
791 Folkes, C.B., de Silva, S.L., Schmitt, A.K., Cas, R.A.F., 2011. A reconnaissance of U-Pb zircon ages in
792 the Cerro Galán system, NW Argentina: prolonged magma residence, crystal recycling, and crustal
793 assimilation. Journal of Volcanology and Geothermal Research 206: 136–147.
794 Förster, H.J., Tischendorf, G., Trumbull, R.B., 1997. An evaluation of the Rb vs. (Y+ Nb) discrimination
795 diagram to infer tectonic setting of silicic igneous rocks. Lithos 40 (2), 261–293.
796 Frost, B.R., Barnes, C.G., Collins, W.J., Arculus, R.J., Ellis, D.J., Frost, C.D., 2001. A geochemical
797 classification for granitic rocks. J. Petrol. 42, 2033‑2048.
798 Ganade, C.E., Lanari, P., Rubatto, D., Hermann, J., Weinberg, R.F., Basei, M.A.S., Tesser, L.R.,
799 Caby, R., Agbossoumonde, Y., Ribeiro, C.M., 2021. Magmatic flare-up causes crustal thickening at
800 the transition from subduction to continental collision. Commun. Earth Environ. 2 (41).
801 Gasquet, D., Roger, J., Chalot-Prat, F., Hassenforder, B., Baudin, T., Chèvremont, P., Razin, P.,
802 Benlakhdim, A., Mortaji, A., Benssaou, M., 2001. Notice explicative carte géol. Maroc (1/50 000),
803 feuille Tamazrar, Notes et Mémoires Serv. Géol. Maroc, n°415 bis, MEM/BRGM. Carte géologique
804 par Roger, J., Gasquet, D., Baudin, T., Chalot-Prat, F., Hassenforder, B., Marquer, D.,
805 Chèvremont, P., Berrahma, A., Destombes, J. Razin, P., Benlakhdim, M., 2001.
806 Gasquet, D., Levresse, G., Cheilletz, A., Azizi-Samir, M.R., Mouttaqi, A., 2005. Contribution to a
807 geodynamic reconstruction of the Anti-Atlas (Morocco) during Pan-African times with the emphasis

on inversion tectonics and metallogenic activity at the Precambrian-Cambrian transition. Precambrian Research 140, 157–182. https://doi:10.1016/j.precamres.2005.06.009.

Gasquet, D., Ennih, N., Liégeois, J-P., Soulaimani, A., Michard, A., 2008. The Panafrican belt. In: Michard A., Saddiqi O., Chalouan A., Frizon de Lamotte D. (Eds.), Continental Evolution: The Geology of Morocco. Structure, Stratigraphy, and Tectonics of the Africa-Atlantic-Mediterranean Triple Junction, Springer Verl., Berlin, Heidelberg, pp. 33–64.

Geyer, G., 1990. Proposal of formal lithostratigraphical units for the Terminal Proterozoic to early Middle Cambrian of southern Morocco. Newsl. Stratigr. 22 (2/3), 87–109.

Grunder, A.L., Klemetti, E.W., Feeley, T.C., McKee, C.M., 2008. Eleven million years of arc volcanism at the Aucanquilcha Volcanic Cluster, northern Chilean Andes: implications for the life span and emplacement of plutons. Transactions of the Royal Society of Edinburgh: Earth Sciences 97: 415–436.

Hassenforder, B., 1987. La tectonique panafricaine et varisque de l'Anti-Atlas dans le massif du Kerdous, Maroc. Thèse Doctorat ès-Sciences, Université Louis Pasteur, Strasbourg, 249 p.

Hassenforder, B., Roger, J., Baudin, T., Chalot-Prat, F., Gasquet, D., Berrahma, A., Chèvremont, P., Marquer, D., Razin, P., Benlakhdim, M., 2001. Carte géol. Maroc (1/50 000), feuille Sidi Bou'addi. Notes et Mémoires Serv. Géol. Maroc, n°414.

Hawkins, M.P., Beddoe-Stephens, B., Gillespie, M.R., Loughlin, S., Barron, H.F., Barnes, R.P., Powell, J.H., Waters, C.N., Williams, M., 2001. Carte géologique du Maroc au 1/50 000, feuille Tiwit. Notes et Mémoires du Service Géologique du Maroc 404.

Hefferan, K., Soulaimani, A., Samson, S.D., Admou, H., Inglis, J., Saquaque, A., Latifa, C., Heywood, N., 2014. A reconsideration of Pan African orogenic cycle in the Anti-Atlas Mountains, Morocco. J. Afr. Earth Sci. 98, 34–46. https://doi.org/10.1016/j.jafrearsci.2014.03.007

Hildebrand, R.S., Whalen, J.B., 2014. Arc and slab-failure magmatism in Cordilleran batholiths II – The Cretaceous Peninsular Ranges Batholith of southern and Baja California. Geoscience Canada, 41, 399–458. https://doi.org/10.12789/geocanj.2014.41.059

Hildebrand, R.S., Whalen, J.B., 2017. The tectonic setting and origin of Cretaceous batholiths within the North American Cordillera: The case for slab failure magmatism and its significance for crustal growth. Geological Society of America Special Paper 532, 113 p. https://doi:10.1130/2017.2532.

Hildebrand, R.S., Whalen, J.B. and Bowring, S.A. 2018. Resolving the crustal composition paradox by 3.8 billion years of slab failure magmatism and collisional recycling of continental crust. Tectonophysics, 734–735, 69–88. https://doi.org/10.1016/j.tecto.2018.04.001

Hollard, H., Choubert, G., Bronner, G., Marchand, J., Sougy, J., 1985. Carte géologique du Maroc, échelle: 1/1.000.000. Notes Mém. Serv. Géol. Maroc, n°260.

Ikenne, M., Soderlund, U., Ernst, R., Pin, C., Youbi, N., El Aouli, E.H., 2017. A c. 1710 Ma mafic sill emplaced into a quartzite and calcareous series from Igherm, Anti-Atlas, Morocco: evidence that the Taghdout passive margin sedimentary group is nearly 1 Ga older than previously thought. J. Afr. Earth Sci. 127, 113–135. https://doi:10.1016/j.jafrearsci.2016.08.020.

Inglis, J.D., MacLean, J.S., Samson, S.D., D'Lemos, R.S., Admou, H., Hefferan, K., 2004. A precise U-Pb zircon age for the Bleïda granodiorite, Anti-Atlas, Morocco: implications for the timing of deformation and terrane assembly in the eastern Anti-Atlas. J. Afr. Earth Sci. 39, 277–283. https://doi:10.1016/j.afrearsci.2004.07.041.

Karaoui, B., Breitkreuz, C., Mahmoudi, A., Youbi, N., 2014. Physical volcanology, geochemistry and basin evolution of the Ediacaran volcano-sedimentary succession in the Bas Draâ inlier (Ouarzazate Supergroup, Wtesern Anti-Atlas, Morocco. J. Afr. Earth Sci. 99, 307–331. https://doi:10.1016/j.afrearsci.2014.06.022.

Karaoui, B., Breitkreuz, C., Mahmoudi, A., Youbi, N., Hofmann, M., Gärtner, A., Linnemann, U., 2015. U-Pb ages from volcanic and sedimentary rocks of the Ediacaran Bas Draâ inlier (Anti-Atlas Morocco): Chronostratigraphic and provenance implications. Precambrian Res. 263, 43–58. https://doi:10.1016/j.precamres.2015.03.003.

Kouyaté, D., Söderlund, U., Youbin N., Ernst, R., Hafid, A., Ikenne, M., Soulaimani, A., Bertrand, H., El Janati, M., R'kha Chaham, K., 2013. U-Pb baddeleyite and zircon ages of 2040 Ma, 1650 Ma and 885 Ma on dolerites in the West African Craton (Anti-Atlas inliers): Possible links to break-up of Precambrian supercontinents. Lithos 174, 71–84. https://doi:10.1016/j.lithos.2012.04.028.

Leblanc, M., 1975. Ophiolites précambriennes et gîtes arseniés de cobalt (Bou Azzer - Maroc). Ph.D. Dissertation. Paris, France, Université de Paris VI, 329 pp.

Lipman, P.W., Prostka, H.J., Christiansen, R.L., 1971. Evolving subduction zones in the western United States, as interpreted from igneous rocks. Science 174, 821–825.

Pelleter, E., Cheilletz, A., Gasquet, D., Mouttaqi, A., Annich, M., El Hakour, A., Deloule, E., Féraud, G., 2007. Hydrothermal Zircons: A tool for ion microprobe U-Pb dating of gold mineralization (Tamlalt-Menhouhou Gold deposit - Morocco). Chemical Geology 245: 135–161.

Lima, S.M., Corfu, F., Neiva, A.M.R., Ramos, J.M.F., 2012. Dissecting complex magmatic processes: an in-depth U-Pb study of the Pavia Pluton, Ossa-Morena Zone, Portugal. Journal of Petrology 53: 1887–1911.

Lipman, P.W., Prostka, H.J., Christiansen, R.L., 1972. Cenozoic volcanism and plate-tectonic evolution of the western United States. I. Early and Middle Cenozoic. Philosophical Transactions of the Royal Society of London A 271: 217–248.

Maacha, L., Azizi-Samir, M.-R., Bouchta, R., 1998. Gisements cobaltifères du district de Bou Azzer (Anti-Atlas). Structure, minéralogie et conditions de genèse. Chron. Rech. Minière, 531-532, 65–75.

Manea, V.C., Leeman, W.P., Gerya, T., Manea, M., Zhu, G., 2014. Subduction of fracture zones controls mantle melting and geochemical signature above slabs. Nat. Commun. 5, 1–10.

Michard, A., Soulaimani, A., Ouanaimi, H., Raddi, Y., Ait Brahim, L., Rjimati, E., Baidder, L., Saddiqi, O., 2017. Saghro Group in the Ougnat Massif (Morocco), an evidence for a continuous Cadomian basin along the northern West African Craton. C. R. Geoscience 349, 81–90. https://doi:10.1016/j.crte.2017.01.001.

Mortaji A., Ikenne M., Gasquet D., Barbey P., Stussi J. M., 2000. Les granitoïdes paléoprotérozoïques des boutonnières du Bas Drâa et de la Tagragra d'Akka (Anti-Atlas occidental, Maroc) : un élément du puzzle géodynamique du craton ouest- africain. J. African. Earth Sci., 31: 523–538. https://doi:10.1016/S0899-5362(00)80005-6.

Mrini Z., 1993. Chronologie (Rb-Sr, U-Pb), traçage isotopique (Sr-Nd-Pb) des sources des roches magmatiques éburnéennes, panafricaines et hercyniennes du Maroc. Thèse Doctorat es Sciences, Université Cadi Ayad, Marrakech, 227 p.

Noble, D.C., 1972. Some observations on the Cenozoic volcano-tectonic evolution of the Great Basin, western United States. Earth Planet. Sci. Lett. 17, 142–150.

O'Connor, E.A., 2010. Geology of the Draâ, Kerdous, and Boumalne Districts, Anti-Atlas, Morocco. Technical Report IR/10/072, British Geological Survey, Keyworth, Nottingham, England.

Ouguir, H., Macaudiere, J., Dagallier, G., 1996. Le protérozoïque supérieur d'imiter, Saghro oriental, Maroc: un contexte géodynamique d'arrière-arc. Journal of African Earth Sciences 22, 173–189. https://doi:10.1016/0899-5362(96)00002-4.

Piqué, A., 2003. Evidence for an important extensional event during the latest proterozoic and earliest paleozoic in morocco. C. R. Geosci. 335, 865–868.

Piqué, A., Bouabdelli, M., Soulaimani, A., Youbi, N., Iliani, M., 1999. The Late Proterozoic III conglomerates of tthe Anti-Atlas (southern Morocco). Their relationships with the Panafrican orogeny or a Late Proterozoic rifting episode. Comptes Rendus de l'Académie des Sciences 328, 409–414. https://doi:10.1016/S1251-8050(99)80107-4.

Roger, J., Gasquet, D., Baudin, T., Chalot-Prat, F., Hassenforder, B., Marquer, D., Chèvremont, P., Berrahma, A., Destombes, J. Razin, P., Benlakhdim, M., 2001. Carte géol. Maroc (1/50 000), feuille Tamazrar. Notes et Mémoires Serv. Géol. Maroc, n°415.

Roger, J., Chèvremont, P., Razin, P., Thiéblemont, D., Baudin, T., Calvès, G., Anzar-Conseil, 2005. Notice explicative, carte géol. Maroc (1/50 000), feuille Tlatat Ida Gougmar, Notes et Mém. Serv. Géol. Maroc, n°498bis, MEM/BRGM, 105 p. Carte géol. par Calvès G., Gabudianu D., Chèvremont P., Roger J., Razin P., (2005), Notes et Mém. Serv. Géol. Maroc, n°498.

Saquaque, A., Benharref, M., Abia, H., Mrini, Z., Reuber, I., Karson, J. A., 1992. Evidence for a Panafrican volcanic arc and wrench fault tectonics in the Jbel Saghro, Anti-Atlas, Morocco. Geologische Rundschau 81, 1–13.

Schwartz, J.J., Klepeis, K.A., Sadorski, J.F., Stowell, H.H., Tulloch, A.J., Coble, M.A., 2017. The tempo of continental arc construction in the Mesozoic Median Batholith, Fiordland, New Zealand. Lithosphere 9, 343–365.

Skilling, I.P., 1994. Evolution of an englacial volcano: Brown Bluff, Antarctica. Bull Volcanol 56, 573–591.

Smellie, J.L., Skilling, I.P., 1994. Products of subglacial volcanic eruptions under different ice thickness: two examples from Antarctica. Sedimentary Geology 91, 115–129.

Soulaimani, A., Bouabdelli, M., Piqué, A., 2003. L'extension continentale au Néoprotérozoïque supérieur – Cambrien inférieur dans l'Anti-Atlas (Maroc). Bull. de la Société Géologique de France 174, 83–92. https://doi:10.2113/174.1.83

924 Soulaimani, A., Essaifi, A., Youbi, N., Hafid, A., 2004. Les marqueurs structuraux et magmatiques de
925 l'extension crustale au Protérozoïque terminal-Cambrien basal autour du massif de Kerdous (Anti-
926 Atlas occidental, Maroc). C. R. Geoscience 336, 1433–1441. https://doi:10.1016/jcarte.2004.03.020
927 Soulaimani, A., Blein, O., Chèvremont, Ph., Ouanaimi, H., Hafid, A., Admou, H., Baudin, T.,
928 Bouabdelli, M, Razin, Ph., Abia, E.H., Beni Akhy, R., 2013. Notice explicative carte géol. Maroc
929 (1/50 000), feuille Agadir Melloul, Notes et Mémoires Serv. Géol. Maroc, n°549, MEM/BRGM.
930 Carte géologique par Blein, O., Roger, J., Chèvremont, Ph., Baudin, T., Soulaimani, A., Ouanaimi,
931 H., Admou, H., Hafid, A., Abia, E.H., Bouabdelli, M., 2013.
932 Soulaimani, A., Ouanaimi, H., Michard, A., Monterod, P., Bead, F., Corsini, M., Molinad, J.-F., Rjimati,
933 E.-C., Saddiqig, O., Hefferan, K., 2019. Quartzite crests in Paleoproterozoic granites (Anti-Atlas,
934 Morocco); a hint to Pan-African deformation of the West African Craton margin. J. Afr. Earth Sci.
935 2019; 157(February):103501. https://doi:10.1016/j.jafrearsci.2019.05.009.
936 Sun, S.S., McDonough, W.F., 1989. Chemical and isotopic systematics of oceanic basalts:
937 implications for mantle composition and processes. In: Saunders, A.D., Norry, M.J. (Eds.),
938 Magmatism in the Ocean Basins, 42 (Special publication). Geological Society, 313–345.
939 Thomas, R.J., Chevallier, L.C., Gresse, P.G., Harmer, R.E., Eglington, B.M., Armstrong, R.A., de
940 Beer, C.H., Martini, J.E.J., de Kock, G.S., Macey, P., Ingram, B., 2002. Precambrian evolution of
941 the Siroua Window, Anti-Atlas Orogen, Morocco. Precambrian Research 118, 1–57.
942 https://doi:10.1016/S0301-9268(02)00075-X.
943 Thomas, R.J., Fekkak, A., Errami, E., Loughlin, S.C., Gresse, P.G., Chevallier, L.P., Liégeois, J.-P.,
944 2004. A new lithostratigraphic framework for the Anti-Atlas Orogen, Morocco. Journal of African
945 Earth Sciences, 39, pp. 217–226. https://doi:10.1016/j.jafrearsci.2004.07.046.
946 Toummite, A., Liégeois, J.-P., Gasquet, D., Bruguier, O., Beraaouz, E.H., Ikenne, M., 2012. Field,
947 geochemistry and Sr-Nd isotopes of the Pan- African granitoids from the Tifnoute Valley (Sirwa,
948 Anti-Atlas, Morocco): a post-collisional event in a metacratonic setting. Mineral. Petrol. 107 (5),
949 739–763. https://doi:10.1007/s00710-012-0245-3.
950 Tuduri, J., Chauvet, A., Barbanson, L., Bourdier, J.L., Labriki., M., Ennaciri, A., Badra, L., Dubois, M.,
951 Ennaciri-Leloix, C., Sizaret, S., Maacha, L., 2018. The Jbel Saghro Au(-Ag, Cu) and Ag-Ah
952 metallogenetic province: Product of a long-lived Ediacaran tectono-magmatic evolution in the
953 Morocan Anti-Atlas. Minerals 8, 592. https://doi:10.3390/min8120592.

954 Walsh, G.E., Aleinikoff, J.N., Benziane, F., Yazidi, A., Armstrong, T.R., 2002. U-Pb zircon
955 geochronology of the Paleoproterozoic Tagragra de Tata inlier and its Neoproterozoic cover,
956 western Anti-Atlas, Morocco. Precambrian Research 117, 1–20. https://doi:10.1016/S0301-
957 9268(02)00044-X
958 Walsh, G.J., Benziane, F., Aleinikoff, J.N., Harisson, R.W., Yazidi, A., Burton, W.C., Quick, J.E.,
959 Saadane, A., 2012. Neoproterozoic tectonic evolution of the Jebel Saghro and Bou Azer-El Graara
960 inliers, eastern and central Anti-Atlas, Morocco. Precambrian Res. 216-219, 23–62.
961 https://doi:10.1016/j.precamres.2012.06.010.
962 Whalen, J.B., Hildebrand, R.S., 2019. Trace element discrimination of arc, slab failure, and A-type
963 granitic rocks. Lithos 248-349, 105179. https://doi:10.1016/j.lithos.2019.105179.
964 Yajioui Z., Karaoui, B., Chew, D., Breitkreuz, C., Mahmoudi, A., 2020. U-Pb zircon geochronology of
965 the Ediacaran volcano-sedimentary succession of the NE Saghro inlier (Anti-Atlas, Morocco):
966 Chronostratigraphic correlation on the northwestern margin of Gondwana. Gondwana Res., 87,
967 263-277. https://doi:10.1016/j.gr.2020.06.015.
968 Youbi, N., 1998. Le volcanisme « post-collisionnel »: un magmatisme intraplaque relié à des panaches
969 mantelliques. Etude volcanologique et géochimique. Exemples d'application dans le
970 Néoprotérozoïque terminal (PIII) de l'Anti-Atlas et le Permien du Maroc. (PhD thesis). Université de
971 Marrakech
972 Youbi, N., Kouyaté, D., Söderlund, U., Ernst, R.E., Soulaimani, A., Hafid, A., Ikenne, M., El Bahat, A.,
973 Bertrand, H., Rkha Chaham, K., Ben Abbou, M., Mortaji, A., El Ghorfi, M., Zouhair, M., El Janati,
974 M., 2013. The 1750 Ma magmatic event of the West African Craton (Anti-Atlas), Morocco.
975 Precambrian Res. 236, 106–123. https://doi:10.1016/j.precamres.2013.07.003.

976 **Tables**

977 **Table 1:** Variation contents of REEs in the Tagragra-n-Daouizid rhyolites.

978 **Table S1:** Representative chemical analyses of volcanic rocks from Tagragra Ouhallal.

979 **Table S2:** Representative chemical analyses of volcanic rocks from Tagragra-n-Daouizid.

980 **Table S3:** Representative chemical analyses of volcanic rocks from south Kerdous inlier.

	Tagraga-n-Daouizid rhyolites			
	Group I	**Group II**	**Group III**	**Group IV**
$[La/Yb]_n$	20 - 60	25 - 36	8 - 17	1.5 - 22
$[Yb]_n$	<5	<10	>10	<10
$[La/Sm]_n$	2.7 - 8.9	4.4 - 5.0	3.0 - 4.1	2.3 - 4.1
$[Gd/Yb]_n$	2.8 - 8.3	2.8 - 4.5	1.6 - 3.0	0.9 - 2.9
Eu anomalie	negative	no	light negative	light negative
ΣREE ppm	75 - 200	165 -210	185 -300	35 -55

Highlights

- An Upper Ediacaran felsic pyroclastic magmatism, the Ouarzazate Group
- Felsic rocks generated by partial melting of crustal lithologies.
- Rare mafic rocks evolve from calc-alkaline to continental tholeiitic affinities.
- Few intermediate and felsic rocks characteristics of slab failure context.

Declaration of competing interest

The authors declare that they have no known competing financial interests or personal relationships that could have appeared to influence the work reported in this paper.